CONF-78-166-5
E-0313
C78/01/16

ADVANCES IN THE STUDY OF SPIN EFFECTS IN NUCLEON-NUCLEON SCATTERING AT SMALL AND INTERMEDIATE MOMENTUM TRANSFERS*

by

Homer A. Neal
Department of Physics
Indiana University
Bloomington, Indiana 47401

*Work supported by the U.S. Department of Energy under contract E(11-1)2009, Task A.

Invited paper presented at the 1978 Orbis Scientiae, Center for Theoretical Studies, University of Miami, Coral Gables, Florida.

Introduction

There has been remarkable progress made in the field of high energy physics in the past few years. We have recently witnessed the discovery of new quantum numbers, the spectra of particles associated with these quantum numbers, and a much improved understanding of the role that all quantum numbers play in high energy interactions. With the wide assortment of experiments and studies being conducted in high energy physics at any one time, it is very easy for one to get the impression that the activity in the field is highly unfocused. On the one hand, it is precisely this apparent unfocused nature that has given rise to much of the excitement and richness of the field. On the other hand, as one examines the situation more closely, one finds that much of the effort in the field is indeed directed toward the solution of a few central problems. One of these problems which I will continually refer to today is that of understanding the details of the structure of the elementary particles. This problem--one of the most fascinating and most difficult problems ever tackled by man--can be approached from several different angles.

For many years, it was felt that the study of polarization phenomena perhaps had little or no bearing on the perceived central problem of the constituent structure of the elementary particles. Recent developments, however, indicate that the study of spin effects may be a very powerful and effective tool for gaining information on the details of particle structure. Major technological advances such as the acceleration of polarized protons, the improvement in polarized targets, and the development of sophisticated polarimeters now make it possible for extremely complicated spin experiments to be carried out with high accuracy. Indeed, we are presently standing at the threshold of being able to extract the precise effect of a particle's spin on its interaction probability at energies of several GeV.

Because of the general complexity of polarization phenomena, even the most rudimentary theoretical understanding of the experimental observations has typically lagged behind the experimental work by a period of many years. Indeed, it is frequently the case that experimentalists will measure the polarization in a certain reaction long before the theoretical description of the differential cross-section has been satisfactorily carried out. During my talk today, however, I will point out what may be an exception to this trend. As we shall see, one of the striking discoveries in recent years has been the observation of significant polarizations in inclusive processes. I will discuss today what appears to be a successful theoretical attempt to explain the observed inclusive polarizations which, in my estimation, illustrates that polarization studies can be an effective tool in the generation and testing of production models.

In my talk, I will begin by reviewing the new developments in elastic scattering processes. This will include a survey of new developments in p-p and n-p elastic scattering cross sections, polarization, and higher order spin measurements. We will then review the existing evidence for a new dibaryon resonance and also examine recent data and theoretical analyses of inclusive baryon polarizations. Next, I will discuss a constituent model of p-p elastic polarization and then, finally, examples will be given to illustrate the status of the program to determine the scattering amplitudes.

Formalism

In an earlier talk at the conference the matter of notation has been taken up so I will keep my comments in this section brief. There are, in principle, sixteen distinct quantities to be measured for a spin ½ - spin ½ elastic scattering process since we need to know the amplitude for transitions from each

of four initial spin states into each of four final spin states. It can be shown that the application of the various strong interaction invariance principles permits the problem to be completely specified in terms of only five amplitudes. The common set[1] of five independent s-channel helicity amplitudes is given below:

$\phi_1 = \langle ++ \vert \phi \vert ++ \rangle$	non-flip
$\phi_2 = \langle -- \vert \phi \vert ++ \rangle$	double-flip
$\phi_3 = \langle +- \vert \phi \vert +- \rangle$	non-flip
$\phi_4 = \langle +- \vert \phi \vert -+ \rangle$	double-flip
$\phi_5 = \langle ++ \vert \phi \vert +- \rangle$	single-flip

In certain applications it is more convenient to deal with a set of amplitudes representing definite parity in the t channel. Such a set has been proposed by Halzen and Thomas[2] and is related to the ϕ's as shown below:

$N_o = \frac{1}{2}(\phi_1+\phi_3)$	Natural parity/non-flip
$N_1 = \phi_5$	Natural parity/single-flip
$N_2 = \frac{1}{2}(\phi_4-\phi_2)$	Natural parity/double-flip
$U_o = \frac{1}{2}(\phi_1+\phi_3)$	Unnatural parity/non-flip
$U_2 = \frac{1}{2}(\phi_4+\phi_2)$	Unnatural parity/double-flip.

A shorthand notation has been developed to designate the spin quantity measured in certain experiments. The probability of the elastic scattering process occuring with the beam, target, scattered, and recoil nucleons in specified spin states can be designated as $I(S_{beam}, S_{target}, S_{scattered}, S_{recoil})$. Now, for the various arguments, let us specify the direction of the nucleon spin by one of the following codes:

$\vec{n} \rightarrow$ normal to scattering plane

$\vec{\ell} \rightarrow$ along nucleon momentum (longitudinal vector)

$\vec{s} \rightarrow \vec{n} \times \vec{\ell}$

$o \rightarrow$ direction unspecified

Then we can define some of the standard observables as follows:

$I_o = I(o,o;o,o)$ (the conventional differential cross section)

$I_oA = I(o,\vec{n};o,o)$ (cross section x analyzing power)

$I_oP = I(o,o;\vec{n},o)$ (cross section x polarization)

$I_oD = I(o,\vec{n};o,\vec{n})$ (cross section x depolarization)

$I_oC_{nn} \rightarrow I_oA_{nn} = I(\vec{n},\vec{n};o,o)$ (cross section x spin correlation parameter)

$I_oR = I(o,\vec{s};o,\vec{s})$ (cross section x rotation parameter)

Any observable quantity, such as the cross section I_o, the polarization P, the depolarization D, the spin correlation parameter $C_{nn}(A_{nn})$, etc. can be readily expressed in terms of a set of helicity amplitudes. Some examples are given below.

$$I_o = \frac{d\sigma}{d\Omega} = \tfrac{1}{2}\left\{|\phi_1|^2 + |\phi_2|^2 + |\phi_3|^2 + |\phi_4|^2 + 4|\phi_5|^2\right\}$$

$$I_oP = \mathrm{Im}\left((\phi_5{}^*(\phi_1 + \phi_2 + \phi_3 - \phi_4)\right)$$

$$I_o(1-D) = \tfrac{1}{2}(|\phi_1 - \phi_3|^2 + |\phi_2 + \phi_4|^2)$$

$$I_o(1-C_{nn}) = \tfrac{1}{2}(|\phi_1 - \phi_2|^2 + |\phi_3 + \phi_4|^2)$$

It is very interesting to note from the above relations how the various observ-

ables are sensitive to different amplitudes. For example, violent structure in ϕ_5 may be invisible in I_o but dominant in P.

p-p Elastic Scattering

A. Differential Cross Sections

Before we get too involved with the discussion of spin effects, it would be appropriate to consider the status of knowledge of the differential cross section in p-p elastic scattering. In Fig. 1 one can see that at low energies $d\sigma/dt$ monotonically declines with θ_{cm}. At energies near 10 GeV a secondary minimum develops near $t = -1.0$ $(GeV/c)^2$ and becomes more pronounced as the energy is increased. By the time we have reached ISR energies, this dip has become quite pronounced. The most recent ISR results shown in Fig. 2 illustrates that over a significant range in t beyond the first minimum the cross section is exponential in behavior, from $-t \approx 1.5$ to 8 $(GeV/c)^2$. Such a mapping of the cross section over many orders of magnitude and the spin measurements which we will discuss in later sections certainly have buried in them an enormous amount of information on the proton--if we can only extract it.

B. Polarization in p-p Elastic Scattering at Low Energies

At energies below 1 GeV the polarization in p-p elastic scattering is about as uninteresting as it can be. With kinematic zeros at $\theta_{cm} = 0^o$ and $\theta_{cm} = 90^o$ it smoothly climbs from $P(\theta_{cm}=0)=0$ to a maximum value near $\theta_{cm} = 45^o$ and then falls smoothly to $P(\theta_{cm} = 90^o) = 0$. Of course, it is significant that finite and even large values of polarization exist at all and this point needs to be firmly kept in mind. What is missing at the low energies is the kind of structure in the polarization that we have found to be particularly pertinent to the details of the interaction. This "dullness" in P is one of the principal reasons

this area of study appeared so hopeless ten year ago. But ten year ago we barely had sufficient data to explore $|t|$ values up to .6 $(GeV/c)^2$. Note that $|t|(\theta_{cm} = 90^o) \cong .4\ (GeV/c)^2$ at $P_{LAB} = 1$ (GeV/c) and that any dynamical effects in P are probably completely masked by the Pauli principle as $\theta_{cm} \rightarrow 90^o$. As the energy of study was raised from cyclotron energies into the several GeV range, we began to learn several interesting features about the p-p polarization as described below.

- In the results of Neal and Longo[3] we were able to first observe the functional form of P(t) with t sufficiently far from $t(90^o)$ to detect an apparent dynamical zero in the polarization near $|t| = .7\ (GeV/c)^2$. This zero seems to be an invariant feature of p-p polarization from a few GeV to a few hundred GeV.
- At energies below 20 GeV relative maxima occur in P(t) near $|t| = .3$ and 1.7 $(GeV/c)^2$.
- In general, the magnitude of the polarization at any given t drops with increasing incident energy.

These features are evident in the plots in Fig. 3 covering the momentum region 1-12 GeV/c. With these general trends of the "low" energy data in mind, I would now like to turn to some of the details of the recent high energy measurements.

C. <u>p-p Elastic Polarizations at High Energies</u>

In this section of the talk I would like to take some time to review an experiment performed by the Indiana University group at the Internal Target Area at Fermilab to study the elastic polarization in proton-proton scattering at energies between 20 and 200 GeV/c. The measurements were confined to $|t|$

values of .3, .6, .8, and 1.0 $(GeV/c)^2$. A hydrogen gas jet was pulsed at the instant that the energy of the circulating Fermilab proton beam was at the desired value. The recoil protons resulting from the interaction of the protons of the atomic hydrogen with the circulating accelerated beam were detected in a superconducting spectrometer and analyzed in a second scattering from a carbon analyzing target.

The experimental layout is shown in Fig. 4. Elements Q1, Q2, and M are superconducting quadrupoles and dipoles. The acceptance of the spectrometer is approximately 1.4 msr. and the momentum acceptance is approximately 5%. A typical example of the missing mass distribution taken with the spectrometer is shown in Fig. 5.

Upon exiting the spectrometer the recoil protons enter a carbon polarimeter shown in Fig. 6. The incident trajectory is determined in the polarimeter by proportional chambers PC1-2. The trajectory of the proton after scattering in the carbon target C is determined by proportional chambers PC3-4. Hodoscopes HX and HY were utilized to aid in the filtering of tracks during the reconstruction. The analyzing power of the carbon target was determined in a separate calibration experiment conducted at the Argonne ZGS. Consequently, for the determination of the polarization of the incident recoil proton it is only necessary to determine the left-right scattering asymmetry, $\varepsilon = (L-R)/(L+R)$. The polarization P of the recoil protons is then simply ε/A, where A is the analyzing power determined in the calibration experiment for the particular energy of the recoil proton.

One novel feature of this experiment was the electronic capability to reject the recording of scatters in the carbon target that were not useful for determining proton polarizations. The overwhelming majority of the protons incident on the carbon target would have preferred to pass through the carbon with the scattering of at most a few degrees. Such small angle scatters are

essentially useless for polarization determination and have the effect of introducing substantial deadtime into the data-taking process. In order to avoid this, we constructed a hardware computer that examined the proportional chamber wire status after each trigger and determined if a scatter had occurred through a sufficiently large angle to be of use in the polarization determination. The effectiveness of this device is illustrated in Fig. 7 which is a scatter plot of the scattering angles in the vertical and horizontal directions. The depletion of events in the center of the plot is a direct result of the action of the polarimeter computer. Without the device this region would have been enormously saturated. Numerous tests were conducted to ensure that the polarimeter computer had no effect on the scatters at the larger angles which were used for the determination of the left-right scattering asymmetry.

Some of the tests conducted in the experiment to ensure that no significant instrumental asymmetries remained include the following. A substantial number of pion triggers were recorded and analyzed to detect any evidence of left-right scattering asymmetries. The asymmetry found in these studies was consistent with zero. Furthermore, we had the opportunity to cross-check our measured results with existing data in certain kinematic regions. The agreement found in these cases was satisfactory in all instances. We also were able to determine the up-down scattering asymmetry from the carbon target. This asymmetry, due to the fact that the p-p interaction is a strong interaction and can produce outgoing polarized protons only with the polarization vector normal to the scattering plane, is expected to be zero and was found to be consistent with zero in our data.

The results from the experiment[4] are shown in Fig. 8 along with published low energy data and preliminary data from experiments at FNAL and CERN. We observe in all cases a rapid decline of the polarization at fixed t as one goes

to higher s values. As one goes to higher t values, there is evidence that the polarization in p-p elastic scattering becomes negative. This is an unusual phenomena for p-p elastic scattering. Indeed, from very low energies up to energies of twenty GeV, there has been no indication of the polarization in p-p elastic scattering becoming negative. This has the interesting geometrical interpretation that as one sits at a fixed center of mass angle and watches the emerging recoil proton, one observes that the outgoing proton will spin in one direction at the lower energies and will eventually spin in the opposite direction as the incident energy is increased.

In a recent paper by Pumplin and Kane,[5] the consequences were investigated of the Pomeron having quantum numbers different from the vacuum. In this paper they investigated the effects on nucleon-nucleon polarizations of the consequences of this assumption. Predictions typical of those in their paper are illustrated in Fig. 8 as dashed lines.

The possible contributions of graphs such as

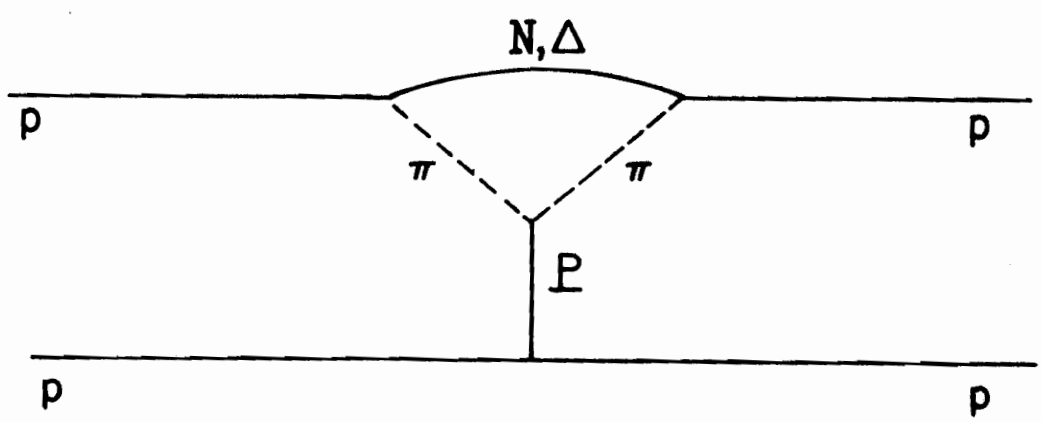

to both the flip (M_{+-}) and non-flip (M_{++}) amplitudes were evaluated. (Here the amplitude subscripts refer to the helicities of the upper vertex protons.) Estimates of the polarization were then obtained by fitting the ISR σ_{tot} and

$d\sigma/dt$ data with the formula

$$M_{++} = is\ 11.5\ Re^{2.21t}\ J_1\ (R\sqrt{-t})/\sqrt{-t} + is\ 1.94\ r^2 e^{3.93t} J_o(r\sqrt{-t}),$$

$$R^2 = 8.47 + .33\ (\ell ns - i\ \pi/2)$$

$$r^2 = 2.92\ (\ell ns - i\ \pi/2)$$

The first term in M_{++} is central in the impact parameter and the second term is peripheral in the impact parameter and is presumably due to the two pion tail contribution. The contribution to the flip amplitude by the two pion graph would then be expected to be of the form

$$M_{+-} = isC\ 1.94\ r^2 e^{3.93t} J_1(r\sqrt{-t})$$

where C is the flip/non-flip ratio calculated from the above graph. Knowledge of M_{++} and M_{+-} permits the calculation of the polarization.

It is of obvious interest that the full implications of this model and its ability to project the general features of high energy polarizations be fully explored.

D. Polarization Due to Coulomb-Nuclear Interference

When one undertakes a study of polarization effects at high energies, it is very important that Coulomb effects are not ignored. This point has been made in a paper by Bourrely and Soffer.[6] They assumed that the non-flip helicity amplitudes received contributions only from the strong interaction and that the single-helicity flip amplitude arises purely from Coulomb effects. In this way they were able to parameterize the polarization resulting from the interference between the Coulomb amplitude and the hadronic amplitude. The maximum value

of the polarization that could arise from this interference effect is shown in Fig. 9 . It is clear from these figures that the interference polarization can be a significant fraction of high energy polarizations.

Depolarization in p-p Elastic Scattering

I would now like to turn my attention to recent results on the depolarization parameter in p-p elastic scattering at energies above 1 GeV. Whereas the polarization parameter in nucleon-nucleon scattering measures the probability for the target particle to become polarized as a result of the elastic scattering process, the depolarization parameter is a measure of the change in the polarization of the target particle that is due to its interaction with the incident nucleon. It has been only very recently that technology has permitted the measurement of the depolarization parameter in p-p elastic scattering at energies at several GeV. The required experiment is made difficult by virtue of the fact that two spins are involved. The standard experimental technique utilizes a polarized proton target to establish the polarization of the target particle and the use of a carbon polarimeter to measure the polarization of the recoil protons. Knowledge of the target polarization, the polarization of the recoil proton, and the polarization parameter for the interaction permits the calculation of the depolarization parameter D. If the recoiling proton has essentially the same polarization as the polarization of the target proton, the depolarization proton has a value near unity.

The depolarization parameter D can be related to the helicity amplitudes mentioned earlier in the talk through the formula given below:

$$I_o(1-D) = \tfrac{1}{2}\,(|\phi_1 - \phi_3)^2 + |\phi_2 + \phi_4|^2).$$

It is clear from this relation that D is sensitive to a different combination of amplitudes than the polarization parameter and , in fact, can represent an independent constraint on the proton-proton system.

Next, let us examine the status of the experimental data on the measurement of the depolarization parameter in p-p elastic scattering at 6 GeV/c. The first high energy t distribution of the depolarization was measured at the Argonne ZGS a few years ago by the Indiana University group[7] (Abshire et al.). At that time there was also a measurement at $t = -.5$ $(GeV/c)^2$ by a Michigan-Argonne-CERN-St. Louis group[8] (Fernow et al.). Since that time substantially more accurate data have become available in experiments by the Michigan-Argonne-CERN-St. Louis group[9] (Ratner et al.) and by the Minnesota group.[10] The situation at 6 GeV/c is shown in Fig. 10. The characteristics of the data are that at small t the depolarization is indeed very close to unity. As one goes to larger t there seems to be a general decline of the polarization--reaching a value of roughly 40% for $|t|$ in the vicinity of 1.0.

If D were actually unity it would imply that

$$\phi_1 = \phi_3$$

$$\phi_2 = \phi_4 .$$

These results are indeed expected at small t since the combinations $\phi_1 - \phi_3$ and $\phi_2 + \phi_4$ can receive contributions only from unnatural parity exchanges and such exchanges are believed, on the basis of independent evidence, to be vanishingly small for the p-p system.

Thus, the p-p depolarization parameter seems to be rather well understood at the moment and to be consistent with rather general theoretical expectations. It will, of course, be of great interest to pursue the depolarization measurements

to higher momenta. In fact, such measurements have been made in the E61 experiment at Fermilab and we can look forward to seeing those results in the near future.

Higher Order Spin Measurements in p-p Elastic Scattering

Much of the progress made in the study of spin effects in p-p elastic scattering at energies below 20 GeV during the past year has been in the area of the higher order spin parameters C_{nn}, $C_{ss}\left[\rightarrow I(\vec{s},\vec{s};o,o)\right]$, and $C_{\ell\ell}\left[\rightarrow I(\vec{\ell},\vec{\ell};o,o)\right]$.

Fig. 11 shows the present status of knowledge of C_{nn} from 2 GeV/c to 12 GeV/c.[11,12] The variation in magnitude and shape over this range is impressive. The structure at 12 GeV/c is particularly notable and this is one of the major effects to surface in the last year--it is begging for an interpretation. How can a proton care so much (dynamically) about which direction the other's spin is pointing?

Another major advance in the study of the p-p system over the past year has been the extraction of accurate data on C_{ss} and $C_{\ell\ell}$ by the Yokosawa group at Argonne.[12] The present status of these measurements is illustrated in Fig. 12. Such measurements are absolutely essential to the process of extracting the various spin amplitudes, as will be seen in a later section.

Neutron-Proton Polarization Data

For many years the subject of neutron-proton polarization at high energies was essentially ignored and most of the effort was concentrated on studying the proton-proton system. The reason for this was simple. Neutrons are harder to produce, transport, polarize, detect, and analyze than are protons. Over the years, however, these problems have been overcome and we have just witnessed the accumulation of a rather substantial amount of high quality neutron-proton

cross section data and polarization data. I will now spend some time briefly reviewing the status of these data.

The proton-proton system is in a pure isospin state of I = 1. Consequently, no amount of studying of this system can reveal any information on the I = 0 amplitudes. The n-p system, on the other hand, is a mixture of I = 1 and I = 0. Therefore, in principle, the combination of the complete n-p and p-p data will permit the isolation of the I = 0 and I = 1 amplitudes. Fig. 13 shows the n-p differential cross section from 5 GeV to 12 GeV taken in an experiment at the Argonne ZGS by a University of Michigan group.[13] One observes that at each energy there is a forward diffraction peak, then a fall-off with increasing t that is somewhat less gradual, a rather flat region as one approaches large angles, and then a rising cross section as one approaches the backward peak. Note that it is meaningful to talk about the differential cross section in n-p elastic scattering beyond 90° in the center of mass since in this case we do not have the complication of identical particles as in the p-p case. Fig. 14 shows the results of measurements by this same Michigan group[14] in an experiment at Fermilab which extended the measurements to 370 GeV/c. The general features are the same: A diffraction peak, and a change in slope in the vicinity of 1 to 1.5 GeV/c. At present we are a long way from understanding all that these measurements are trying to tell us. One feature, however, that is noticeable is that because of the similarity of the slope of the forward diffraction peak in the n-p and p-p cases the radius of interaction of the p-p and n-p systems are essentially the same and are approximately one fermi. Next let us take a look at the situation with the polarizations. The Argonne Effective Mass Spectrometer group[15] has, over the past few years, studied spin effects in both p-p and n-p elastic scattering from 2 to 12 GeV/c. The incident proton beam utilized in these experiments was polarized parallel or anti-parallel to the normal of the scattering

plane. The incoming beam was incident on either neutrons or protons in a deuterium target. The results from these experiments are shown in Fig. 15. One notices that at 2 GeV/c the p-p and p-n polarizations are almost the same--but not quite. As we go from 2 GeV/c to higher momenta, the p-n polarization changes structure at a rather impressive rate. At 12 GeV/c the p-p polarization remains at about .05 over the t range explored while the p-n polarization has essentially vanished over this entire region.

In an optical model one would expect the polarization for p-p and p-n elastic scattering to be identical in shape. In a Regge model one would expect mirror symmetry just as is observed in the case of π^+p and π^-p elastic scattering. It is clear from the data presented above that neither one of these cases pertains exactly for p-p and p-n polarization. There is the general trend of moving from an optical type model at the lower energies to a Regge type picture at the higher energies.

If we designate the non-flip diffractive amplitude by N_o^o and calculate the components of the flip amplitude N_1^I orthogonal to N_o^o as follows:

$$N_{1_\perp}^{o} = \left[(P\sigma)_{pp} + (P\sigma)_{pn} - \tfrac{1}{2}\,(P\sigma)_{cex}\right]/(4|N_o^o|)$$

$$N_{1_\perp}^{1} = \left[(P\sigma)_{pp} - (P\sigma)_{pn}\right]/(4|N_o^o|, \text{ where}$$

$$|N_o^o|^2 \approx (\sigma_{pp} + \sigma_{pn})/2,$$

we can display the single flip amplitudes for each of the two isospin states as a function of P_{LAB} at fixed values of t.[15] This is shown in Fig. 16. One is struck by the rapid fall-off of the I = 0 amplitude and this is the subject of a significant amount of current theoretical activity. One possible explanation of this

effect requires a low lying Regge trajectory given by $\alpha = -.5 + .9t$. The rapid variation of N_1^0 can not be explained as being due only to the interference of a normal Regge amplitude with a Pomeron flip contribution.

The Diffraction Region: Where does it end?

For many years the sharp peak in the differential cross section at small t in elastic scattering processes has been attributed to geometric diffraction effects and the corresponding region in t is called the diffraction region. The region beyond the diffraction peak has been loosely called the "large angle" region and has been assumed to be representative of constituent or exchange processes. This point of view has recently been challenged by Sukhatme.[16] Indeed, he claims that the p-p ISR data out to $|t| = 10\ (\mathrm{GeV/c})^2$ may be predominantly diffractive, whereas traditional wisdom would have the diffraction region stopping at $|t| \simeq 2.5\ (\mathrm{GeV/c})^2$. Below we will present his arguments.

The p-p elastic scattering amplitude is frequently parameterized as follows:

$$A(s,t) = P(s,t) + C(s,t)$$

where P(s,t) represents the Pomeron (diffractive) contribution and C(s,t) is the large angle contribution. P is almost purely imaginary, it dominates at small angle and has dip structure. On the other hand, C is assumed to be smoothly varying, due to other than diffractive processes, and approximately real. It is of interest to know where $|P(s,t)| \simeq |C(s,t)|$, for this can give a rough definition of the boundary between the "diffractive" and "large angle" regions. Sukhatme utilized the phase, magnitude derivative relation to determine the value of the phase angle:

$$\phi = \tan^{-1} \frac{\mathrm{Im}A}{\mathrm{Re}A} \simeq \frac{\pi}{2} - \frac{\pi}{4} \frac{d}{d(\ell ns)} \ell n \frac{d\sigma}{dt}$$

using the existing ISR p-p data. The result of this analyticity test is that A is still predominantly imaginary even at large $|t|$. This is then taken as evidence that the diffraction region may extend even out to $|t| = 10\ (\mathrm{GeV/c})^2$ and beyond. It is suggested that perhaps the regimes are separated by fixed θ_{cm} rather than fixed t or p_t.

Sukhatme finds that the ISR data can be accounted for in diffraction models if inelastic diffraction is taken into consideration. This discussion could be relevant to the development of polarization models for the presently accessible $|t|$ range.

Evidence of a Dibaryon Resonance

There has been evidence recently published by Auer et al.[17] in Physics Letters 67B, 113 (1977) for the existence of a resonance in the p-p system. This information is terribly exciting for at least four reasons: 1) the discovery of any resonance is certainly noteworthy, 2) the discovery of a resonance at a lower energy accelerator is particularly exciting these days since it is generally assumed that all such resonances have already been found and that the new frontiers are now at the highest energy machines, 3) there are traditional theoretical reasons why such resonances should not exist, and 4) the new evidence points up the power of utilizing spin as a tool for investigating spectroscopy.

Very good p-p total cross section data has existed in the region of a few GeV's for many years. The general shape of the cross section is illustrated in Fig. 17 . As one can see, one of the most impressive characteristics of this plot is the rapid rise in the total cross section between 1 and 1.5 GeV/c. This rise has been explained by Mandelstam and others as being due to the production

of the N(1238) through a single pion exchange process. The production of the higher isobars such as the N(1512) and the N(1688) appears to be substantially suppressed relative to that of the N(1238). This suppression can be understood in a model where one assumes that the dominant exchange process is that of single pion exchange. There does appear to be a small peak in the total cross section data near 3 GeV/c. This peak is consistent with N(1688) production. Also, there is some evidence for a shoulder near 2 GeV/c that might correspond to the production of the N(1512). Normally, the existence of a particle or resonance in a system reveals itself as a significant peak in the total cross section energy distribution. For example, the resonances associated with the pion-proton system at intermediate energies are evident in Fig. 18. Obviously, there is no such pronounced peaking in the proton-proton system. It is fair to say that until very recently the high energy physics community was quite well-prepared to assume that all of the structure observed in the p-p total cross section could be explained in terms of the opening of various inelastic channels. The opening of various inelastic channels is what is presumed to be responsible for keeping the total cross section at higher energies roughly constant in the face of a declining elastic total cross section.

Now let us take a look at what is new in the proton-proton system as ascertained from total cross section measurements. All of the total cross section measurements that I have referred to earlier were made without regard to the direction of the projectile or target spin. In the experiment that we will discuss, both the spin of the target particle and the incident projectile were controlled. The Argonne polarized proton beam was made incident on a polarized proton target and experimenters in the Yokosawa group measured the total cross section when the two spins were longitudinally aligned and when the

two spins were longitudinally anti-parallel. The experimenters observed that the parallel spin cross section has a peak near 1.5 GeV/c while the anti-parallel spin cross section is relatively flat. Furthermore, at the position of the peak in $\sigma_{\rightrightarrows}$, it is found that $\sigma_{\rightrightarrows}$ is 50% larger than $\sigma_{\rightleftarrows}$ (Fig. 19). This difference is surprisingly large and naturally leads one to question whether or not the effect might be due to the production of a resonance state of the two incident protons. If so, the mass of the dibaryon system would be roughly 2250 MeV. This resonance would have an electric charge of two units and a baryon number of 2.

In our examination of the total cross section for unpolarized beam and target above, we observed that the rapid variation in the region of 1 to 1.5 GeV/c could be explained by the production of the N(1238). It is thus natural to inquire as to whether the observed structure in the polarized cross section could somehow be related to the N(1238). The first problem associated with this interpretation is that the N(1238) would be expected to produce an effect at a momentum lower than 1.5 GeV. Secondly, the N(1238) would be expected to contribute only to the singlet spin state $^1D_2$ rather than in the triplet spin state which contributes to $\sigma_{\rightrightarrows}$. Recall that it is $\sigma_{\rightrightarrows}$ that shows the striking structure. By making a Legendre coefficient analysis of the differential cross sections and polarizations in p-p elastic scatterings in the neighborhood of 1 to 2 GeV/c, the authors find that their observations are consistent with a standard Breit-Wigner resonance in the $^3F_3$ state with a mass of 2250 MeV, a width of 200 MeV, and elasticity of the order of 20%, and with quantum numbers of $J^P = 3^-$.

In my opening remarks in this section I alluded to the fact that such a resonance does not fit the traditional theoretical expectations. I would like to take a few moments now to clarify that statement. The standard quark model has been amazingly successful in accounting for the large variety of particles which have been discovered. The assumed quantum numbers of the quarks are such

that any known meson can be represented as a system of two of the quarks. Furthermore, any observed baryon can be characterized by a group of three of the quarks. It has long been assumed that these are the rules that govern the formation of physical elementary particles. Indeed, very ambitious experimental programs have been mounted to search for particles which did not fit into this classification. Such hypothetical particles were given the name "exotic". To date there has been no conclusive evidence of the existence of exotic elementary particles. Obviously, the existence of a diproton resonance would require an alteration in the way we view the structure of elementary particles. To make up such an object would require more than the minimal number of quarks. One possibility is, of course, the existence of quark molecules and, in fact, some models presently predict the existence of such objects.

Before we leave this topic I would like to spend a few minutes discussing the possible relationship between such a dibaryon resonance and the observed breaks in the fixed angle proton-proton differential cross sections. Several years ago in an Indiana paper by Kammerud et al.[18] we examined the feasibility of explaining breaks we had observed in the fixed angle cross section in terms of dibaryon resonances as a follow-up on suggestions made by Predazzi and Libby.[19] The p-p differential cross sections presented in that paper are illustrated in Fig. 20 and we can see clear evidence for some significant change in the behavior of the cross section at t values near .8, 3.0, and 6.5 GeV/c. We stated that if one assumed that the change in the slope of the fixed angle cross section was due to the crossing of the threshold for the production of a diproton resonance, the mass of the first resonances would be at 2.2 GeV/c^2. This is a remarkable occurrence and may point the way for explaining the structure in the fixed angle cross section. Members of the Indiana group are presently studying this question.

Λ Hyperon Inclusive Polarization Measurements

In an experiment performed by Bunce et al.[20] at Fermilab, significant polarization effects were observed in the inclusive production of Λ hyperons at 300 GeV. The experiment examined lambdas produced at production angles between 0 and 9.5 mrad in the interaction of 300 GeV protons with a Be target. The polarization of the inclusively-produced lambdas was determined from the observation of the lambda decay into protons and pions. The experimental layout is shown in Fig. 21. The proton beam enters from the left, is bent by magnet M1 onto the beryllium target T. Magnet M2 serves as a sweeping magnet to remove charged particles from the beam. V is a decay vacuum area. The pions and protons from the lambda decay are detected by proportional chambers 1-6. Magnet M3 is used to determine the charge and momentum of the decay products. By manipulating the field in magnet M1 and in other magnets not shown in the figure, the experimenters were able to choose eight production angles ranging from -2.5 mrad to +9.5 mrad.

When a lambda hyperon decays into a proton and a pion, the direction of the proton momentum relative to the spin of the lambda in its rest frame is governed by the following formula:

$$\frac{dN}{d\Omega} = (1 + \alpha P\cos\theta)/4\pi,$$

where θ is the angle between the proton momentum and the lambda spin, P is the magnitude of the lambda polarization and $\alpha = .64 \pm .013$. Consequently, an observation of the angular distribution of the proton resulting from the lambda decay is sufficient to permit the determination of the polarization of the parent lambdas.

I will not go into the details of the experimental procedure or the various tests that were made to insure that all observed asymmetries were due to the physical process of lambda production and decay. The interested reader is referred to Physical Review Letters 36, 1113 (1976). The results of studies by this group are illustrated in Fig. 22 (which also includes their 24 and 400 GeV/c results), where the polarization is plotted against the transverse lambda momentum. One sees the very surprising results that, at large p_t, the polarization reaches the value of almost 30%. This result is initially surprising because it is only in rare circumstances that one observes polarization effects above 25% at any energy above a few GeV. Another feature of this result, however, creates a cause for even more excitement. Normally, inclusive processes are thought to occur as a result of many competing and random production mechanisms. It is very difficult to believe that particles can be produced inclusively with large polarization in such an environment. Indeed, the observation of large polarization may be a principle indicator that such production processes take place in an orderly, non-random fashion. There are several questions raised by this experiment that simply must be answered in the near future. For example, does the almost linear increase in polarization with p_t continue until the polarization saturates at unity? How important is the target Be to the results of the experiment? Would the result be the same if the experiment were conducted off of a hydrogen target? What would be the result of a similar experiment conducted on the sigma hyperons? How does the inclusively-produced lambda polarization compare with corresponding proton data? In a later section of the paper, I will have some additional comments to make on these questions as we compare the lambda results with the results obtained in a recent Indiana University experiment at Fermilab.

Polarization in Inclusive Proton Production

The Indiana University group is presently engaged in a program to study the inclusive polarization in $pp \rightarrow pX$ at Fermilab energies. The apparatus being used for these measurements is identical to that described above for the p-p elastic polarization studies in the Internal Target Area at Fermilab. The initial measurements were made using a rotating carbon filament target at incident proton energies of 100, 200, 300, and 400 GeV/c and at a transverse momentum of 1.1 GeV/c and x = .88.

The study of proton inclusive processes is a natural extension of the elastic polarization studies. Indeed, as shown in Fig. 23 , inclusive final states can be viewed as a massive particle recoiling against the observed proton. For x values near 1, the inclusive cross sections can be calculated as the square of a triple Regge amplitude. Spin flip and non-flip terms can interfere in the triple Regge picture to produce a polarization of the observed proton.

The inclusively-produced protons traverse the superconducting spectrometer and are incident on a carbon analyzing target shown in Fig. 6 . The left-right scattering asymmetry of these protons from the carbon analyzer determines the polarization. The analyzing power for the carbon was previously determined in a calibration experiment performed in the Argonne polarized beam. Numerous checks were made to insure that all instrumental asymmetries were cancelled to a high degree.

The results of these measurements[21] are shown in Fig. 24 along with the lambda inclusive polarization results of Bunce et al.[20] One notes that the lambda and proton polarization are of the same sign and are of the same order of magnitude. The curve shown in this figure is a triple Regge prediction of the type predicted by the calculations of Field and Fox, Salin and Soffen, and Paige and Sidhu.[22] The absolute value of the curve is at least a factor of ten greater

than the current prediction of the triple Regge model. The results shown here are not in agreement with the magnitude or energy dependence of any simple triple Regge model. It is interesting to speculate that the proton polarization seen in these measurements may well be related to the large values of the polarization seen in inclusive lambda processes. In the discussion in the next section, we will indeed present a model due to Heller[23] and to Kane and Yao[24] that relates the lambda inclusive polarizations and the proton inclusive polarizations. Before leaving this section, I should comment that we are presently engaged in a major run at Fermilab that should expand the range over which the inclusive proton polarizations are known to higher transverse momenta. It is our hope to have the data from this experiment analyzed by summer.

Theoretical Model of Baryon Inclusive Polarization

In a recent preprint by Ken Heller[23] at the University of Michigan, a mechanism is proposed that allows large polarization for baryons which are fragments of the projectile or target particle. It is assumed that when one of the quarks in the projectile baryon is scattered by a target nucleon, a vector particle is radiated similar to the process that occurs in bremsstrahlung. Further, the radiated particle is assumed to create a quark-antiquark pair. Then one member of this pair joins the other two quarks of the projectile to create the outgoing observed baryon. The process is illustrated in Fig. 25. In this example, we are visualizing the inclusive production of a forward lambda hyperon by an incoming proton. The lambda is produced through the interchange of one of the u-quarks in the incoming proton with an s-quark produced by the radiated vector particle.

If it is assumed that the coupling of the quarks to the appropriate vector gluon is independent of color, one may write the wave functions of spin index i

as

$$P_i = \sqrt{2}\left[u_i u_i d_j - u_i u_j d_i\right]$$

$$\Lambda_i = \sqrt{3}\left[u_i d_j s_i - u_j d_i s_i\right],$$

where j is the other spin index.

For an incident proton to produce an outgoing Λ, the unscattered u and d quarks are assumed to be in a singlet state in the incident proton since these quarks are not affected by the proposed transition mechanism. Therefore, the transition matrix for the production of a spin i lambda by a spin i proton is as follows:

$$\langle \Lambda_i | T | p_i \rangle = \sqrt{6}\Big[\langle u_i d_j s_i | T | u_i d_j u_i \rangle - \langle u_j d_i s_i | T | u_i d_j u_i \rangle$$
$$- \langle u_i d_j s_i | T | u_i d_i u_j \rangle + \langle u_j d_i s_i | T | u_j d_i u_i \rangle\Big].$$

The second and third terms in this expansion are assumed to be negligible since they require spin index changes. Pursuing this calculation leads to the conclusion that, in this model, the polarization of the produced Λ is unity. In this scheme the observation of Λ polarizations smaller than unity would be explained by the dilution created by other competing Λ production processes which decrease in prominence at higher p_t.

This model has other substantial capabilities which we will not investigate in detail here. However, the ratio of polarizations for various baryon production processes is of interest and is reproduced in Fig. 26. One should note that the prediction is that proton inclusive polarization should be approximately one-third smaller than those of the lambda inclusive polarizations. In a more

detailed study by Kane and Yao[24] (University of Michigan Report HE7-44) it is predicted that the polarization in inclusive nucleon production and lambda production are in the ratio of the non-strange and strange constituent quark masses. From the paper of De Rujula et al. (Physical Review D 12, 147 (1975)) this ratio is predicted to be .62. The SU(6) correction calculated by Heller to account for the extent to which one quark carries the spin of the hadron is two-thirds. These two effects should be combined to obtain the actual ratio of the polarization in $pp \rightarrow pX$ vs. $pp \rightarrow \Lambda X$. The result of this process is that the proton polarizations should be a factor of .42 of the inclusive lambda polarizations. Obviously, there is substantial interest in studying the kinematic region over which relations of this type might be expected to hold. For example, it is important to know whether the inclusive polarization for protons rises with p_t in a manner similar to that for lambda inclusive polarizations. Also, over what range of s values does such a correspondence hold? As can be seen from Fig. 27 , the predictions of Heller, Kane, and Yao are remarkably satisfied by the existing data.

Elastic Nucleon-Nucleon Polarization in a Constituent Model

Several years ago in what we believe to be the first attempt to explain the polarization phenomena in a constituent model, Holger Nielsen at the Niels Bohr Institute in Copenhagen and I proposed a scheme to test the dominance of constituent scattering in elastic proton-proton processes.[25] In brief, the model assumed that the various regions of the fixed angle proton-proton differential cross section are due to different numbers of binary parton collisions occurring in the p-p process. If one examines the fixed angle 90° differential cross section as a function of t (Fig. 28), one observes rather distinct breaks near $t=-1$, $t=-3$, and $t= -6.5\ (\mathrm{GeV}/c)^2$. Let us suppose that the first region from $0 < t < 1$ is

due to the single scattering of one parton in the incident proton from one parton in the target proton, with the partons recombining in the final state to produce the outgoing observed protons as shown in Fig. 29. Furthermore, suppose that the region between $t = -1$ and $t = -3$ $(GeV/c)^2$ is due to two partons in the incident proton scattering from two partons in the target proton to produce the p-p elastic scattering process at the observed t. At a given value of t in this second region this double scattering process might be preferred over the one described for region 1 since the two partons can scatter through smaller angles to produce the observed t than would be required for a single parton scatter. The description for region 3 and others would be specified in a similar manner. There is one further ingredient in the model. This is the assumption that the polarization of the outgoing protons is the sum of the polarization of the scattered partons. The basic recurrence relation provided by this model is as follows:

$$P(t) = nS(t/n^2),$$

where n specifies the number of parton collisions taking place, P is the polarization at four momentum transfer squared t, and S is the polarization for parton-parton collisions as determined from proton-proton collisions in region 1.

In order to see if such a relation has any possible validity, one can simply determine S(t) by looking at the polarization in p-p elastic scattering at t values below 1 $(GeV/c)^2$. The value of the predicted polarization in region 2, where two binary parton-parton collisions are assumed to dominate the process, can then be easily generated from the formula above with $n = 2$. The results of this operation are illustrated in Fig. 30 where one sees the agree-

ment to be unusually good. While this model is obviously extremely crude it does raise the possibility that someday we will be able to understand elastic and inclusive polarizations on the basis of the polarization produced by the constituent particles. One notes here certain similarities between this model and the one utilized by Heller in his description of inclusive polarization. Indeed, one of the interesting features that needs to be explored is the relationship between inclusive and elastic polarization in constituent models.

Amplitude Analysis

From a purely mechanistic view one could say that it is the experimentalist's job to make the measurements required to determine the spin amplitudes and it is the theorist's job to find out what the amplitudes are telling us about nature. We do not yet quite have enough information to fully make an unambiguous amplitude determination--but we are getting close. The p-p elastic amplitude situation at 6 GeV/c and $|t| \approx .3$ $(\mathrm{GeV/c})^2$ is shown[12] in Fig.31 . In Fig.31a we see from the shaded region the range of possible values for the amplitudes N_o, N_1, N_2, U_o, U_2 as a result of constraints imposed by σ, P, D_{nn}, C_{nn}, K_{nn}. In Fig. 31b we see the additional improvement due to knowledge of R. The effects of new information on $I(\vec{s},o;o,\vec{s})$ and $I(\vec{s},\vec{n};o,\vec{s})$ is illustrated in Fig.31c. Finally, the effect of adding information on $I(\vec{s},\vec{s};o,o)$ further constrains the amplitudes as shown in Fig.31d. The goal of having only a zero width dot in each amplitude plot is obviously still not achieved but remarkable progress has been made in the past two years and we can realistically look forward to significant successes in this area in the near future.

References

1. M. Goldberger et al., Phys. Rev. 120, 2250 (1960).
2. F. Halzen and G. Thomas, Phys. Rev. D10, 344 (1974).
3. H. A. Neal and M. J. Longo, Phys. Rev. 161, 1374 (1967).
4. M. D. Corcoran et al., p-p Polarizations at High Energies, submitted to Phys. Rev. Lett., 1978.
5. J. Pumplin and G. L. Kane, Phys. Rev. D11, 1183 (1975).
6. C. Bourrely and J. Soffer, Nuovo Cim. Lett. 19, 569 (1977).
7. G. Abshire et al., Phys. Rev. D12, 3393 (1975).
8. R. C. Fernow et al., Phys. Lett. 52B, 243 (1974).
9. L. G. Ratner et al., Phys. Rev. D15, (1977).
10. M. Marshak, private communications, 1978.
11. A. D. Krisch, Nucleon-Nucleon Elastic Scattering at Large P_t^2 and Spin, Review Paper presented at the 1977 APS DPF Meeting, October 1977, Argonne, IL.
12. A. Yokosawa, Proceedings of the Second International Conference on the Nucleon-Nucleon Interaction, Vancouver, Canada (June 1977).
13. J. L. Stone et al., Phys. Rev. Lett. 38, 1315 (1977).
14. C. E. DeHaven et al., Univ. of Mich. preprint UMHE 77-43.
15. S. L. Kramer et al., Polarization Parameter for Nucleon-Nucleon Elastic Scattering at 11.8 GeV/c, ANL-HEP-PR-77-74, 1977. (Previous meas. referenced therein)
16. U. P. Sukhatme, Some New Aspect of High Energy pp Elastic Scattering, Univ. of Cambridge preprint, 1977.
17. I. P. Auer et al., Phys. Lett. 67B, 113 (1977).
18. R. C. Kammerud et al., Phys. Rev. D4, 1309 (1971).
19. L. Libby and E. Predazzi, Nuovo Cim. Lett. 2, No. 18, 881 (1969).
20. G. Bunce et al., Phys. Rev. Lett. 36, 1113 (1976); O. Overseth, private communication, 1978.

21. M. D. Corcoran et al., Preliminary Measurements of Proton Polarization in High Energy Inclusive Processes, Indiana University Internal Report IUHEE #10, 1977.

22. F. E. Paige and D. P. Sidhu, Phys. Rev. D14, 2307 (1976); P. Salin and J. Soffer, CERN Preprint TH 1769-CERN; R. D. Field and G. D. Fox, Nuc. Phys. B80, 367 (1974).

23. K. Heller, A Quark-Gluon Mechanism for Inclusive Polarization, Univ. of Michigan preprint, 1977.

24. G. L. Kane and Y. P. Yao, Studying Gluon Properties Experimentally, Univ. of Michigan prepring UM HE 77-44, 1977.

25. H. A. Neal and H. B. Nielsen, Phys. Lett. 51B, 79 (1974).

Figure Captions

Fig. 1 Differential cross section in p-p elastic scattering (Ref. 18).

Fig. 2 Recent differential p-p cross section measurements at the ISR (Ref. 11).

Fig. 3 Polarizations in p-p elastic scattering from 1 to 12 GeV/c.

Fig. 4 Layout of Indiana University experiment E313 at Fermilab.

Fig. 5 Typical missing mass distribution in experiment E313.

Fig. 6 Layout of carbon polarimeter used in experiment E313.

Fig. 7 Scatter plot of horizontal and vertical scattering angles in experiment E313. Depletion in center represents effect of hardwired polarimeter computer which rejects small angle scatters.

Fig. 8 Results from experiment E313.

Fig. 9 Maximum polarizations vs. t arising from Coulomb interference effects (Ref. 6).

Fig. 10 Depolarization in p-p elastic scattering at 6 GeV/c (Refs. 7-10).

Fig. 11 Measurements of C_{nn} from 2 to 12 GeV/c (Refs. 11, 12).

Fig. 12 Measurements of C_{ss} and $C_{\ell\ell}$ (Ref. 12).

Fig. 13 n-p differential cross sections at Argonne energies (Ref. 13).

Fig. 14 n-p differential cross sections at Fermilab energies (Ref. 14).

Fig. 15 p-p and n-p elastic polarizations from 2 to 12 GeV/c (Ref. 15).

Fig. 16 Dependence of nucleon isospin spin flip amplitudes at fixed t as a function of P_{LAB} (Ref. 15).

Fig. 17 Total cross section in p-p scattering (from Bugg *et al.*, Phys. Rev. *146*, 980 (1966)).

Fig. 18 Pion-proton total cross section features.

Fig. 19 Difference in longitudinal total p-p cross sections; evidence for a dibaryon resonance (Ref. 17).

Fig. 20 Differential p-p cross sections at $\theta_{cm} = 90^{o}$ observed in Indiana University experiment (Ref. 18, 25) divided by exponential in t.

Fig. 21 Experimental layout for inclusive lambda polarization experiment (Ref. 20).

Fig. 22 Results from inclusive lambda polarization experiment (Ref. 20).

Fig. 23 Illustration of proton inclusive process.

Fig. 24 Inclusive proton polarizations observed in Indiana University experiment E313 at Fermilab (Ref. 21).

Fig. 25 Illustration of inclusive model of Heller (Ref. 23).

Fig. 26 Predicted ratio of various inclusive baryon polarizations in model of Heller (Ref. 23).

Fig. 27 Comparison of p and Λ inclusive polarizations.

Fig. 28 Fixed angle (90°) differential cross section in p-p elastic scattering.

Fig. 29 Illustration of parton-parton scattering model of Neal and Nielsen (Ref. 25).

Fig. 30 Fit of model of Ref. 25 to polarization data. The polarization curve in region I generates the curve in region II with no free parameters.

Fig. 31 Present status of knowledge of amplitudes. See text for description.

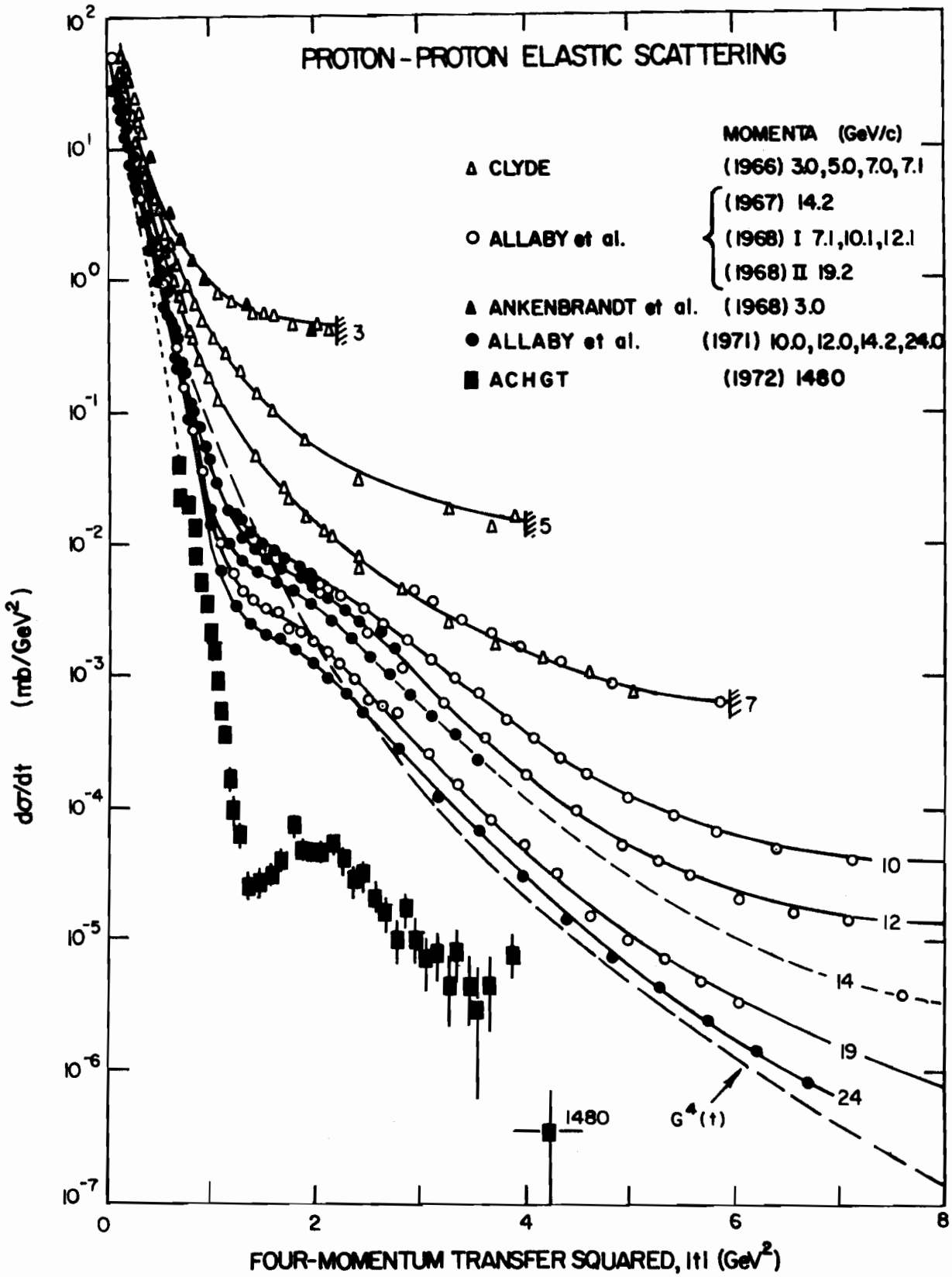
PROTON - PROTON ELASTIC SCATTERING
MOMENTA (GeV/c)
Δ CLYDE (1966) 3.0, 5.0, 7.0, 7.1
○ ALLABY et al. (1967) 14.2
(1968) I 7.1, 10.1, 12.1
(1968) II 19.2
▲ ANKENBRANDT et al. (1968) 3.0
● ALLABY et al. (1971) 10.0, 12.0, 14.2, 24.0
■ ACHGT (1972) 1480
3
5
7
10
12
14
19
24
1480
G⁴(t)
dσ/dt (mb/GeV²)
FOUR-MOMENTUM TRANSFER SQUARED, |t| (GeV²)

Figure 1

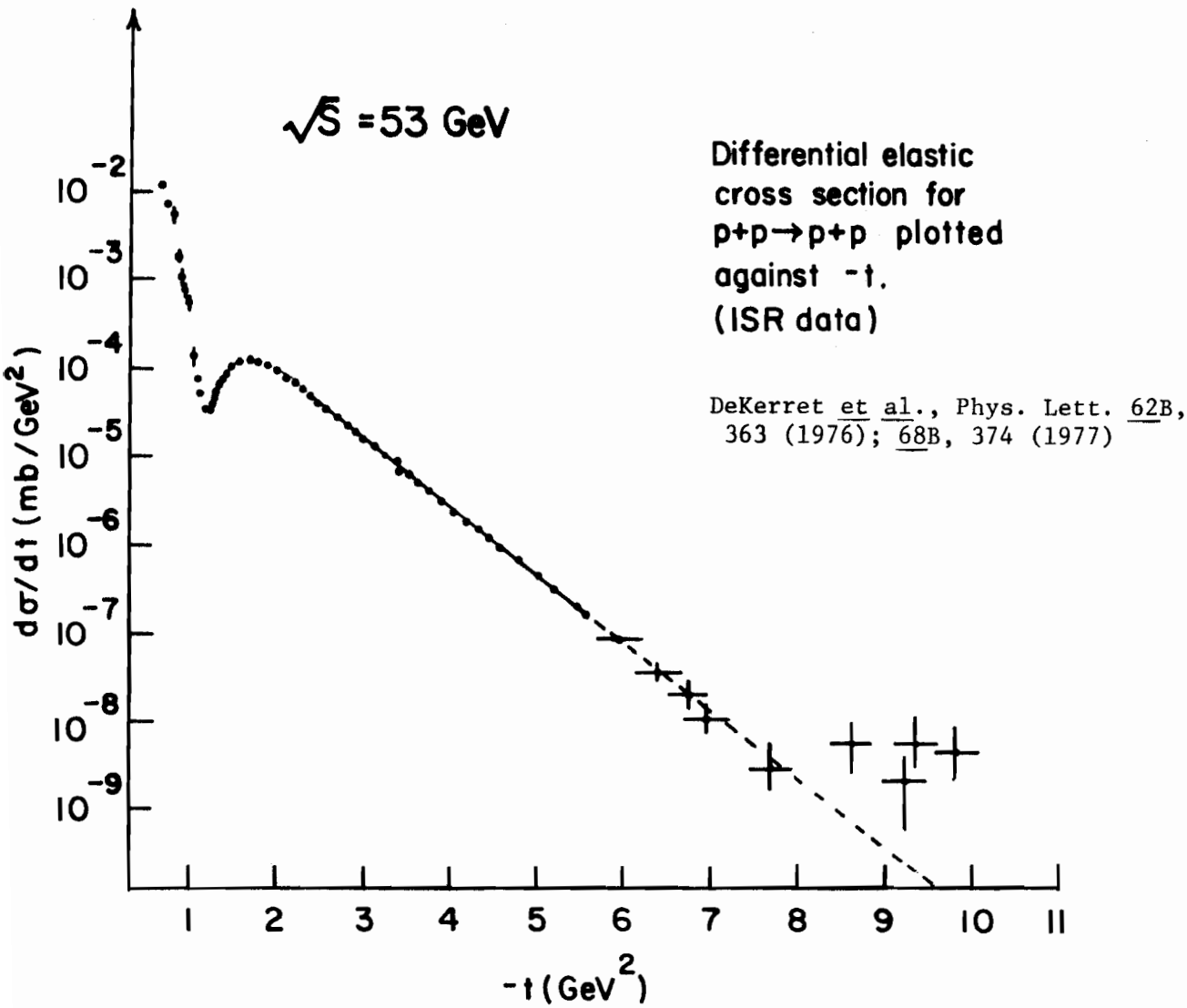
√S =53 GeV
Differential elastic cross section for p+p→p+p plotted against -t. (ISR data)
DeKerret et al., Phys. Lett. 62B, 363 (1976); 68B, 374 (1977)
dσ/dt (mb/GeV²)
10⁻²
10⁻³
10⁻⁴
10⁻⁵
10⁻⁶
10⁻⁷
10⁻⁸
10⁻⁹
1
2
3
4
5
6
7
8
9
10
11
-t (GeV²)

Figure 2

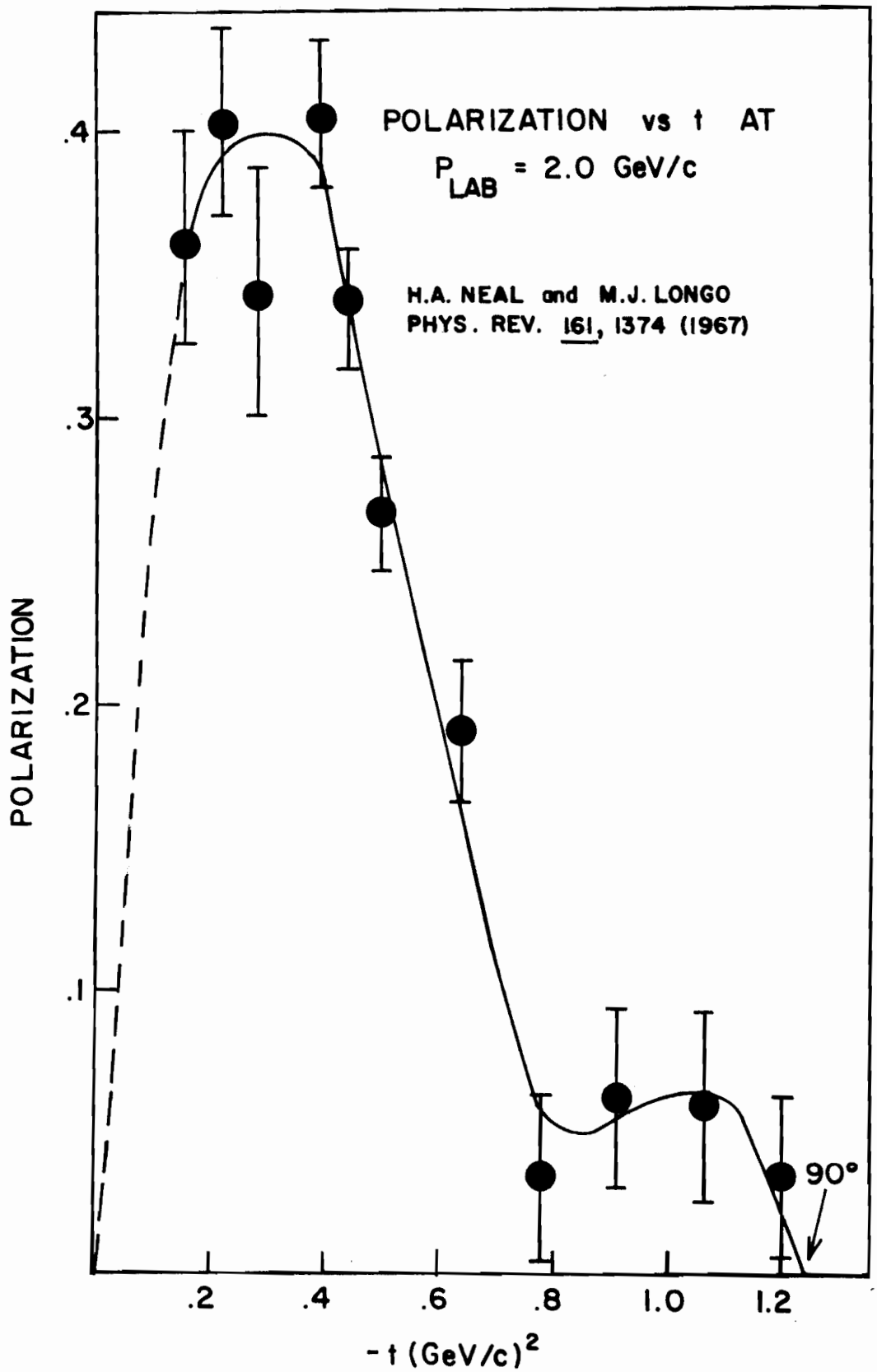
POLARIZATION vs t AT
P_{LAB} = 2.0 GeV/c
H.A. NEAL and M.J. LONGO
PHYS. REV. 161, 1374 (1967)
POLARIZATION
.4
.3
.2
.1
90°
.2
.4
.6
.8
1.0
1.2
$-t\ (GeV/c)^2$

Figure 3A

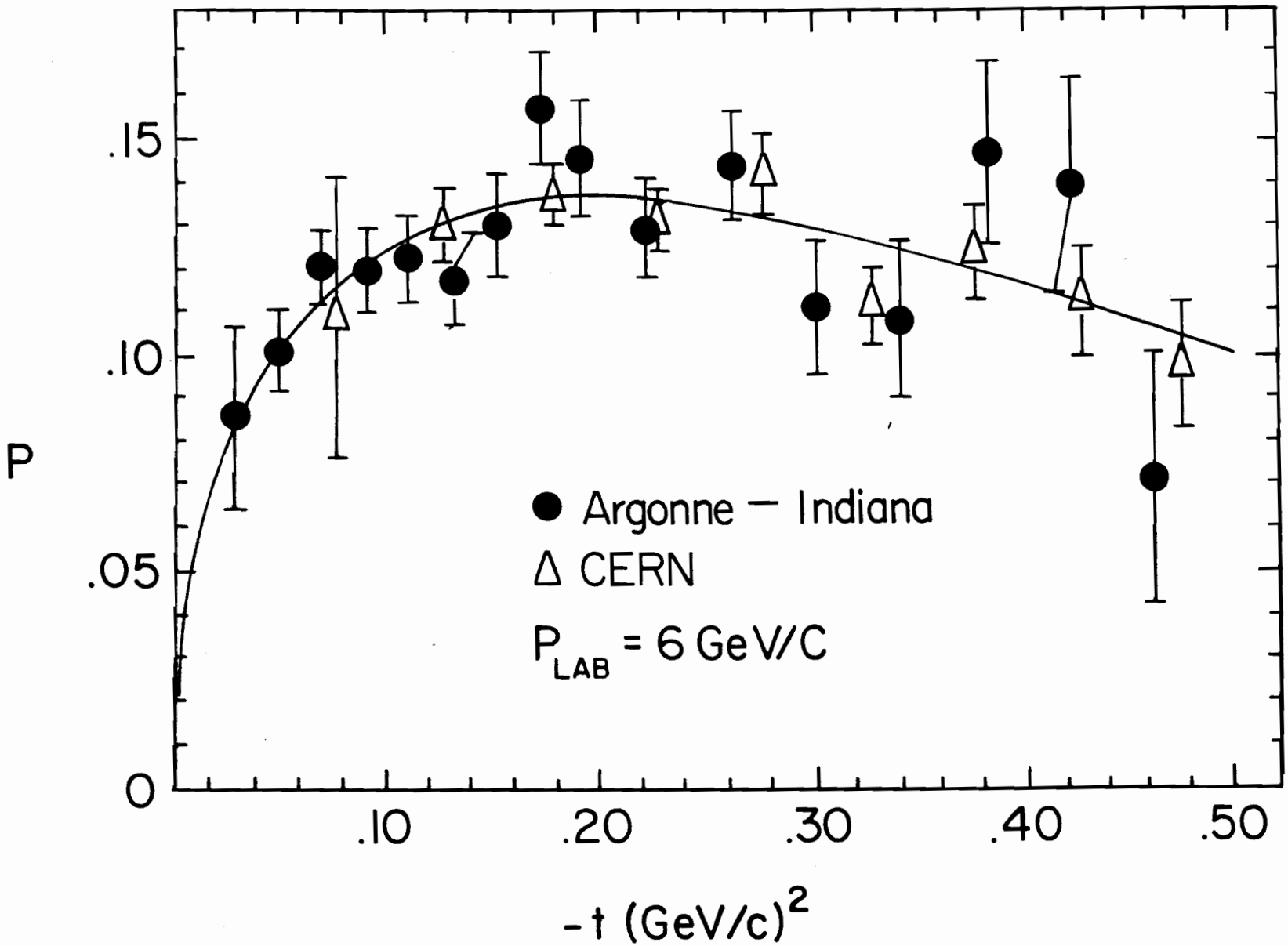
.15
.10
.05
0
P
.10
.20
.30
.40
.50
-t (GeV/c)^2
● Argonne — Indiana
Δ CERN
P_{LAB} = 6 GeV/C

Figure 3B

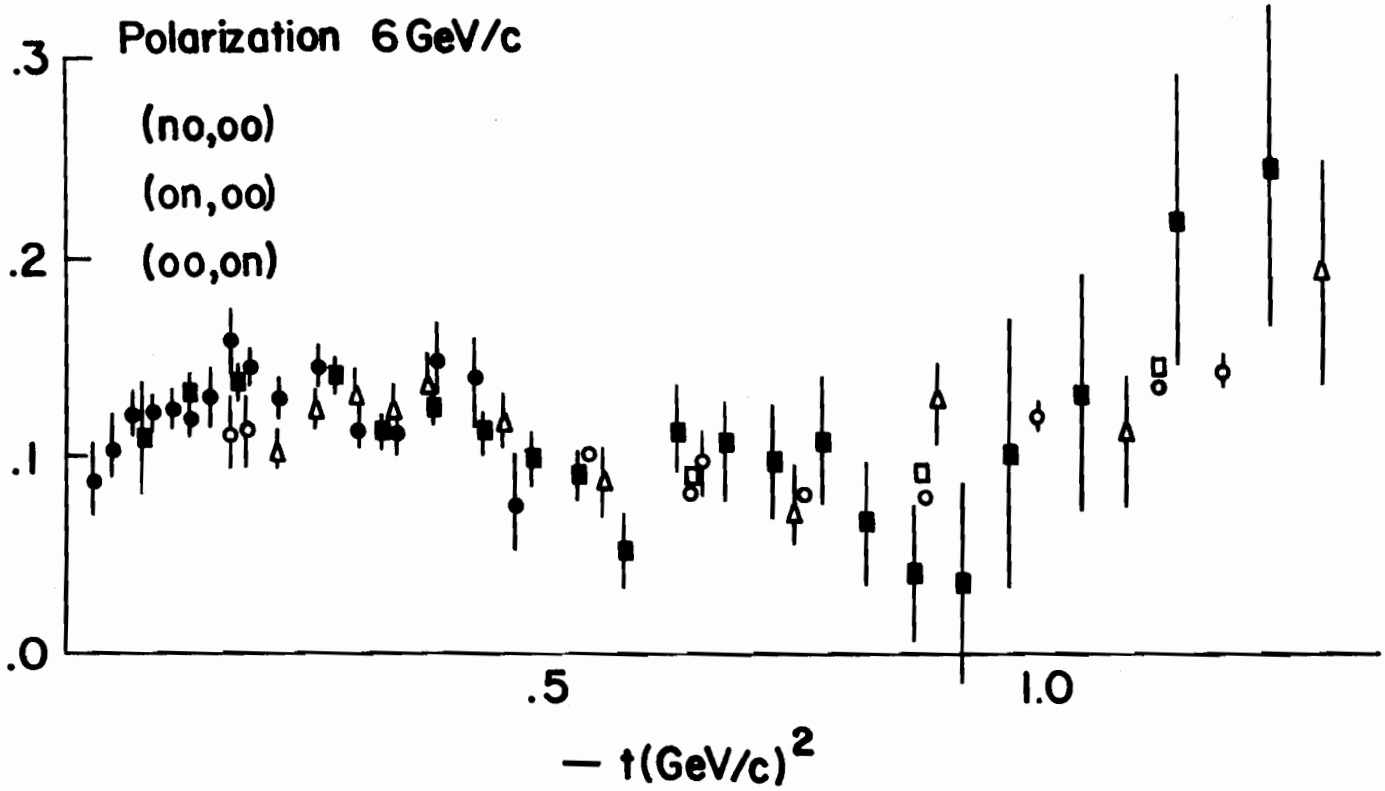

● INDIANA UNIVERSITY - ARGONNE

■ Borghini

△ Diebold et al

○ □ Michigan

Figure 3C

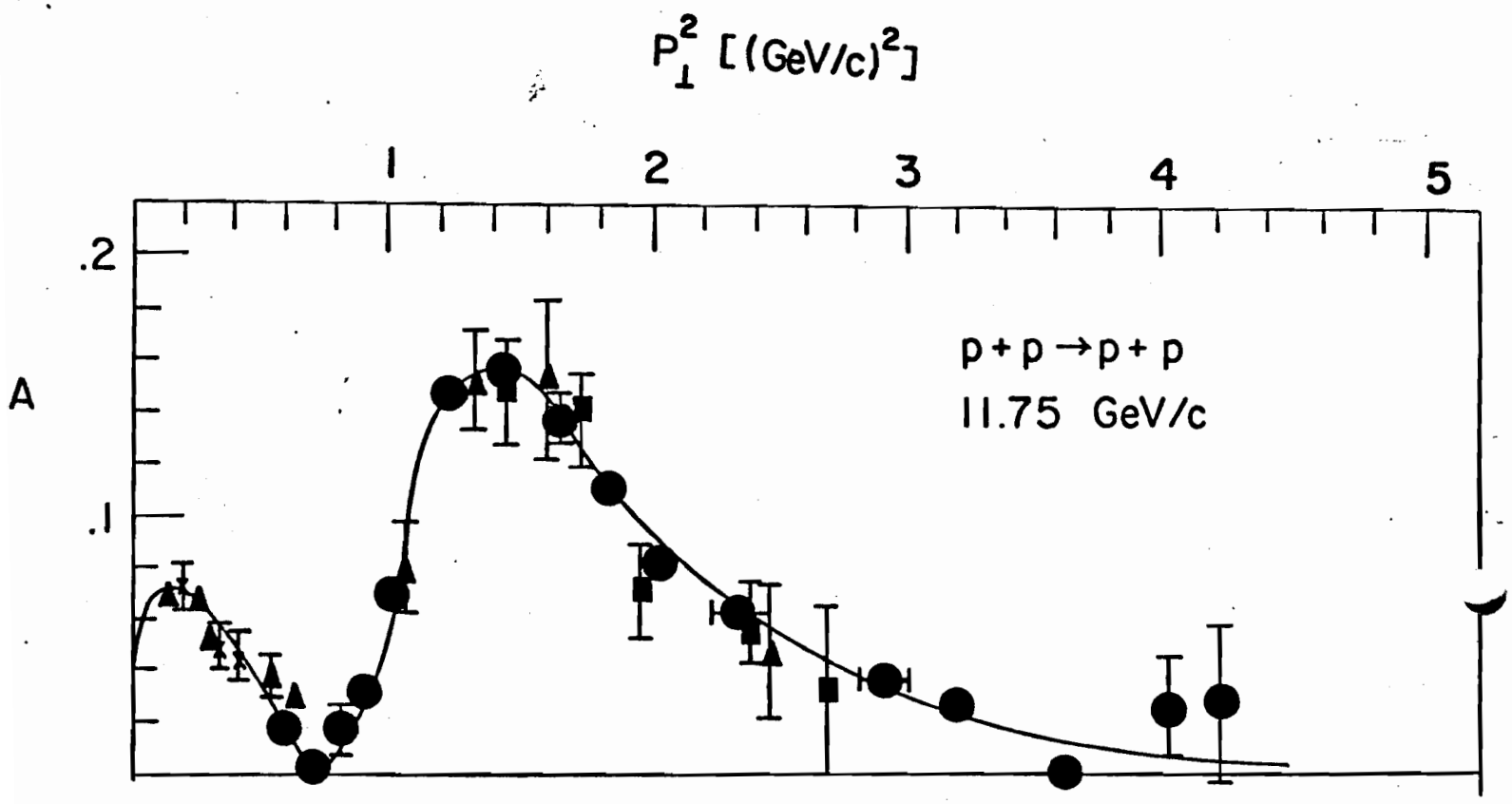

● This exp., Abe et al, Miettinen et al (Michigan)

x Kramer et al (Argonne)

■ Bryant et al 12.33 GeV/c (Indiana)

▲ Borghini et al 10 and 14 GeV/c (CERN) averaged

Figure 3D

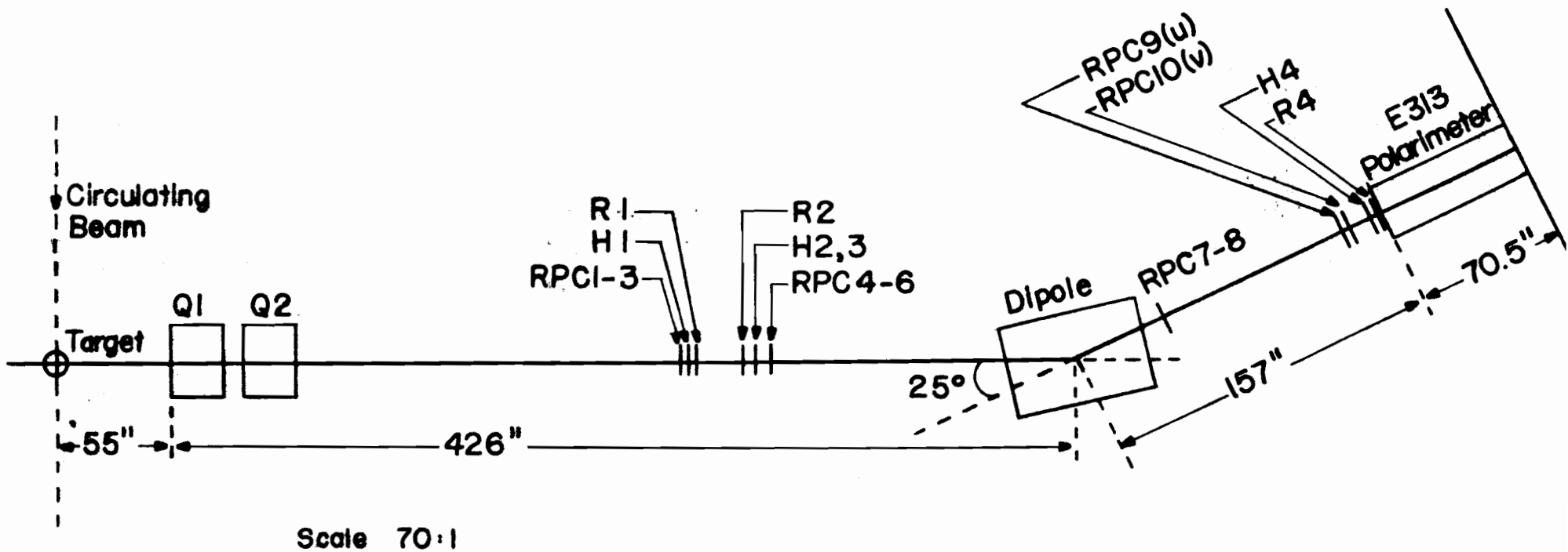

INTERNAL TARGET SPECTROMETER

Figure 4

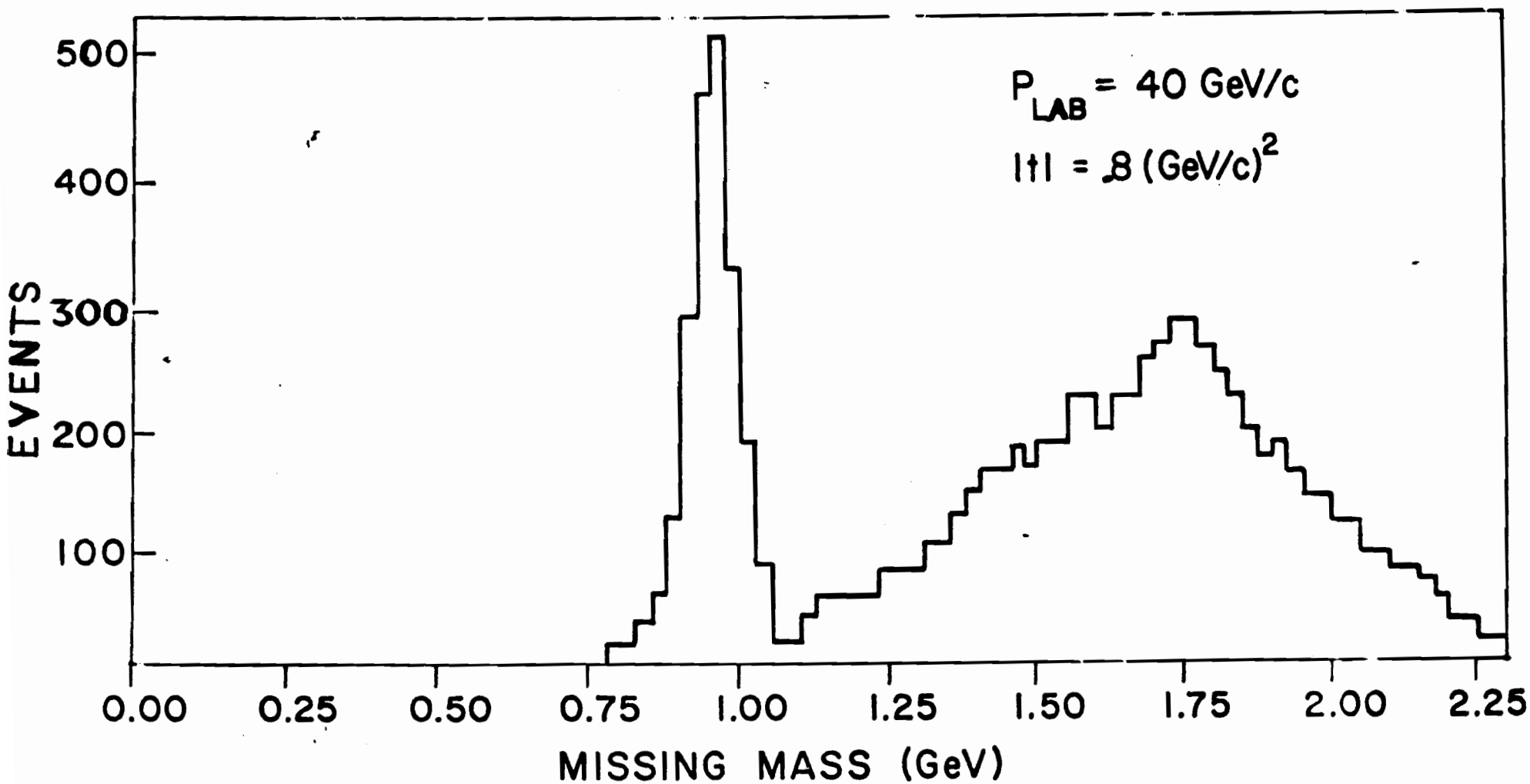
P_{LAB} = 40 GeV/c
|t| = .8 (GeV/c)^2
EVENTS
500
400
300
200
100
0.00
0.25
0.50
0.75
1.00
1.25
1.50
1.75
2.00
2.25
MISSING MASS (GeV)

Figure 5

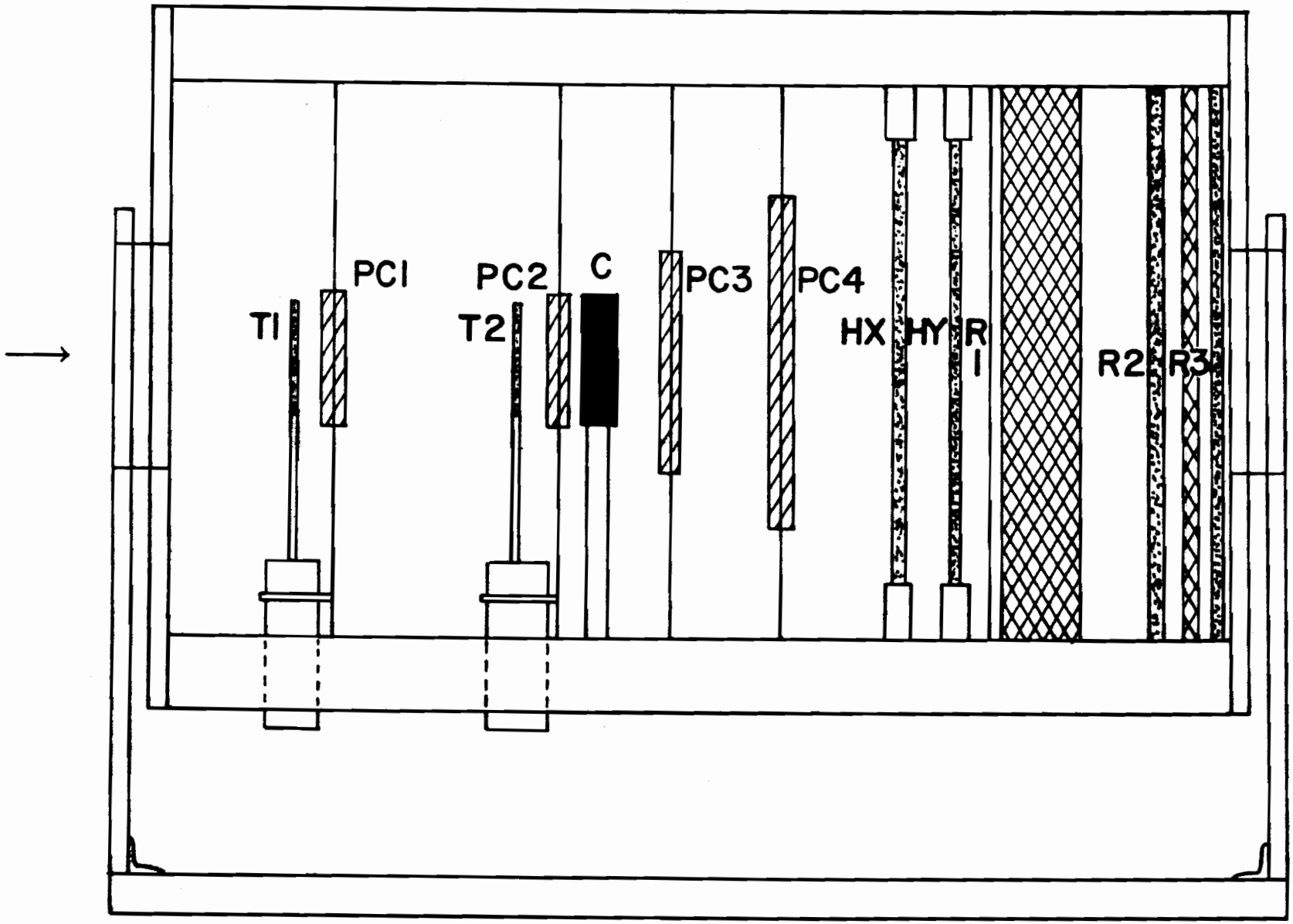

POLARIMETER LAYOUT

scale: 1/8" = 1"

proportional chambers
range steel
scintillation counters
carbon block

Figure 6

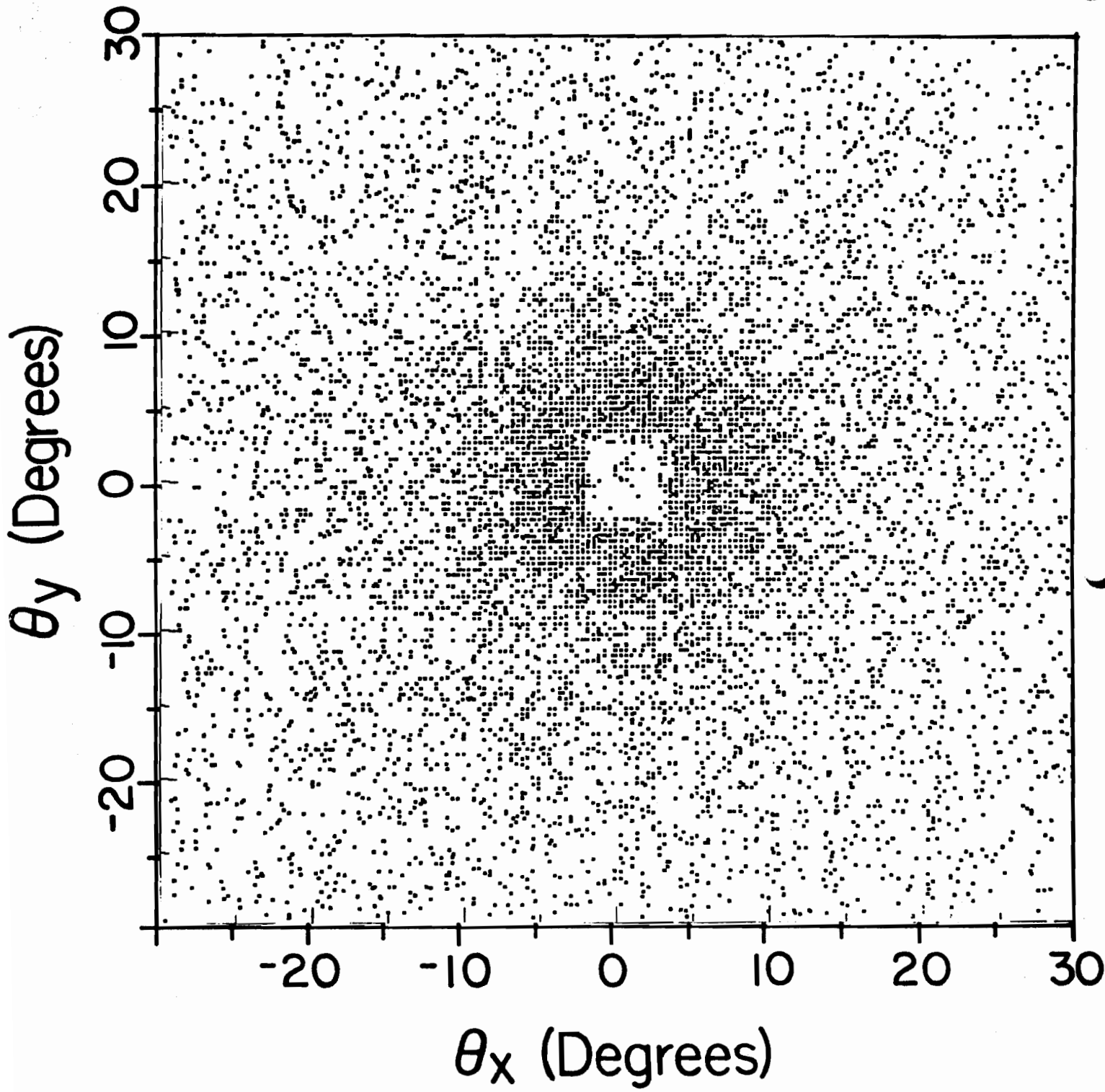

Figure 7

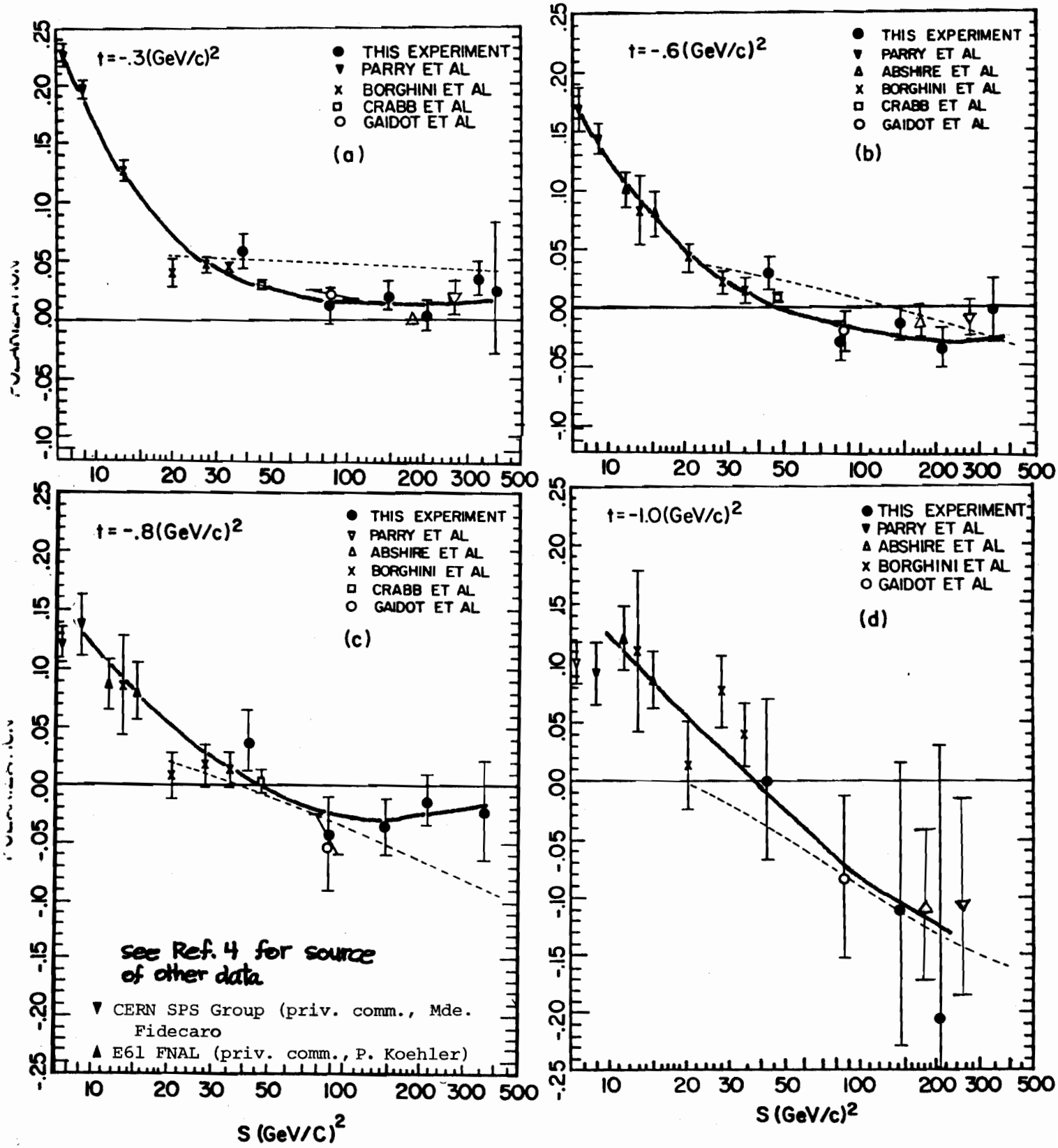
t=-.3(GeV/c)²
THIS EXPERIMENT
PARRY ET AL
BORGHINI ET AL
CRABB ET AL
GAIDOT ET AL
(a)
t=-.6(GeV/c)²
THIS EXPERIMENT
PARRY ET AL
ABSHIRE ET AL
BORGHINI ET AL
CRABB ET AL
GAIDOT ET AL
(b)
t=-.8(GeV/c)²
THIS EXPERIMENT
PARRY ET AL
ABSHIRE ET AL
BORGHINI ET AL
CRABB ET AL
GAIDOT ET AL
(c)
see Ref. 4 for source of other data
CERN SPS Group (priv. comm., Mde. Fidecaro
E61 FNAL (priv. comm., P. Koehler)
t=-1.0(GeV/c)²
THIS EXPERIMENT
PARRY ET AL
ABSHIRE ET AL
BORGHINI ET AL
GAIDOT ET AL
(d)
S (GeV/C)²
S (GeV/c)²

Figure 8

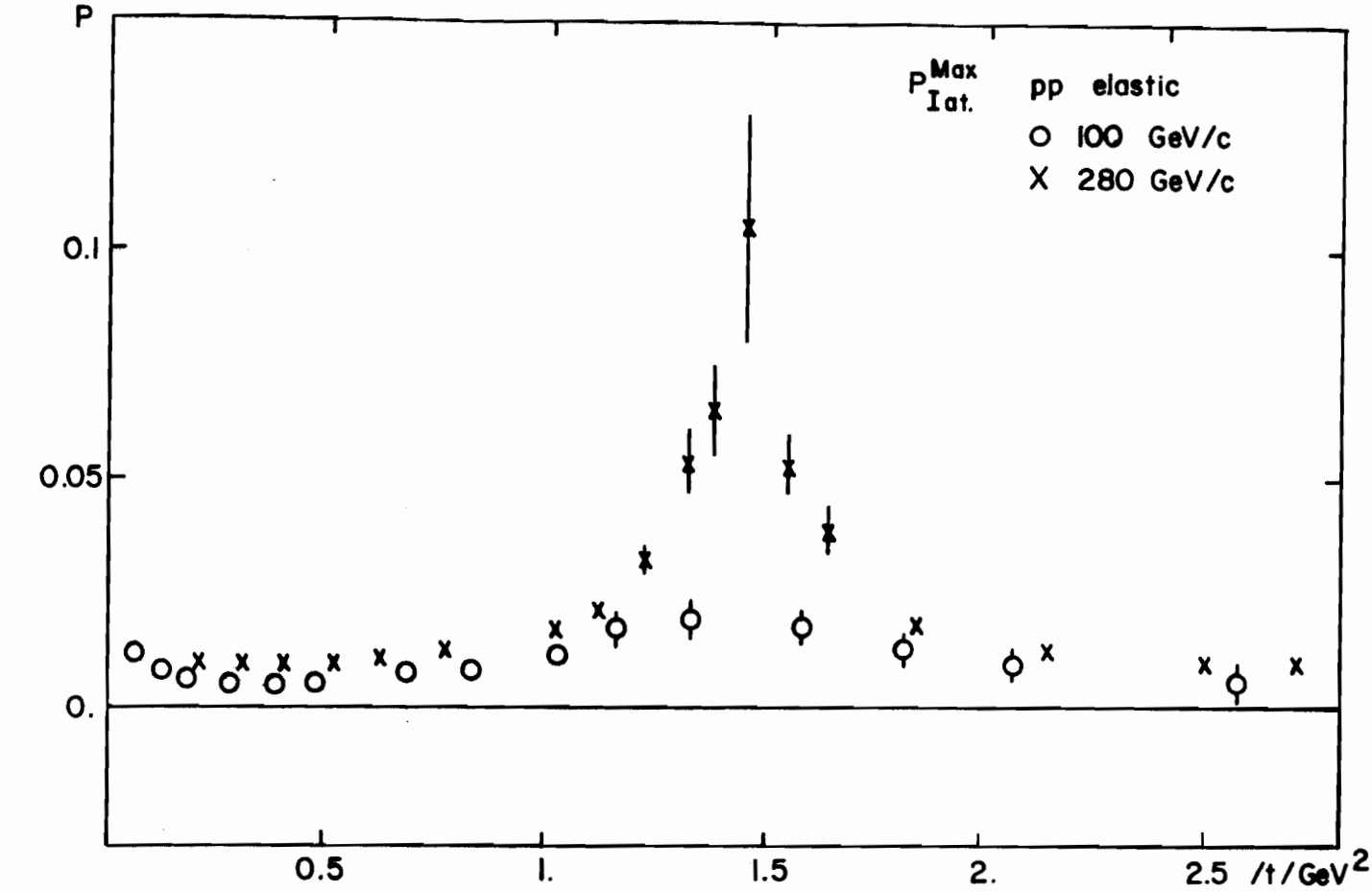
P
$P^{Max}_{Iat.}$
pp elastic
O 100 GeV/c
X 280 GeV/c
0.1
0.05
0.
0.5
1.
1.5
2.
2.5
/t/GeV^2

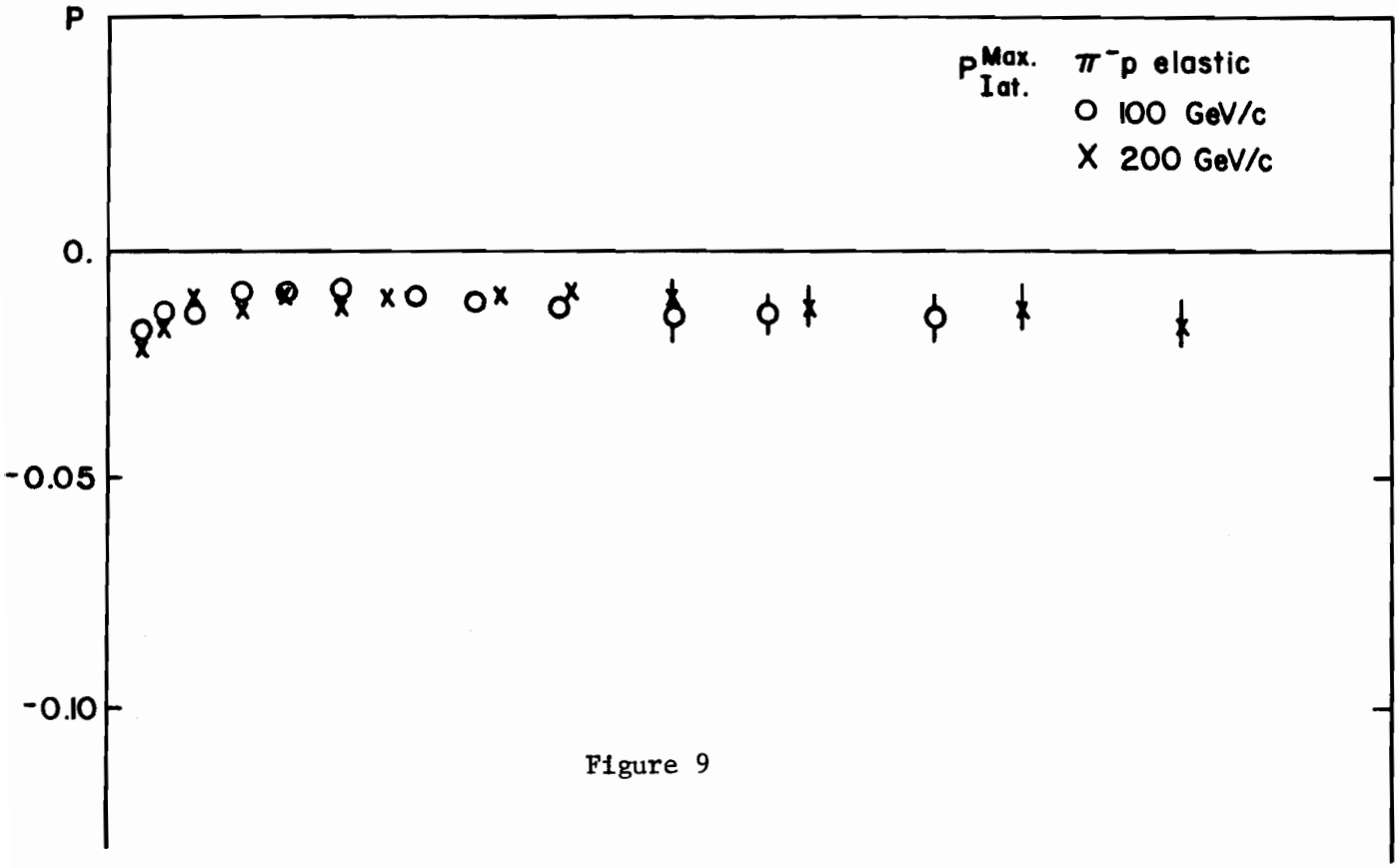
P
$P^{Max.}_{Iat.}$
π^-p elastic
O 100 GeV/c
X 200 GeV/c
0.
-0.05
-0.10

Figure 9

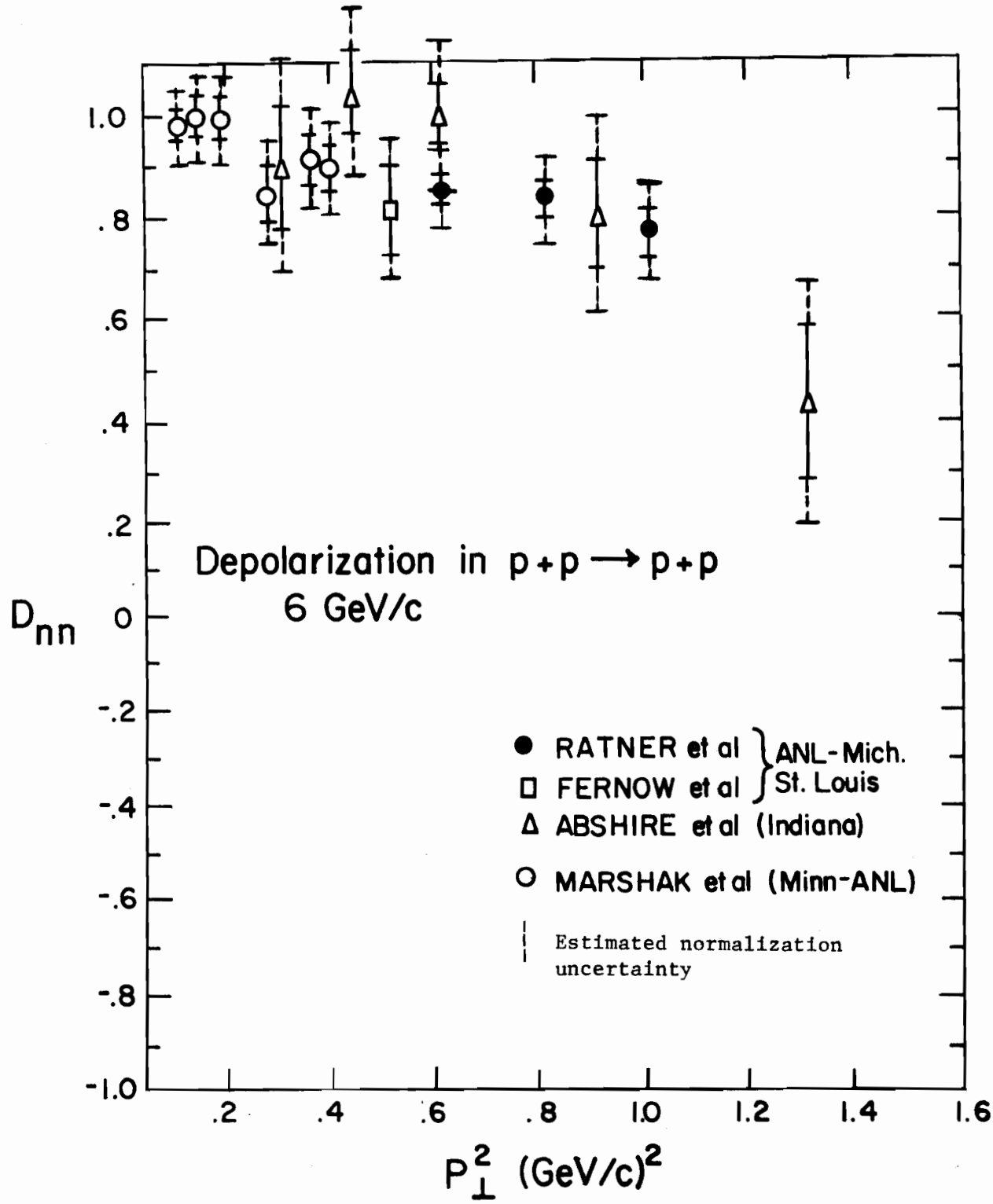
Depolarization in p+p → p+p
6 GeV/c
D_{nn}
1.0
.8
.6
.4
.2
0
-.2
-.4
-.6
-.8
-1.0
.2
.4
.6
.8
1.0
1.2
1.4
1.6
$P_\perp^2$ (GeV/c)^2
RATNER et al
FERNOW et al
ANL-Mich.
St. Louis
ABSHIRE et al (Indiana)
MARSHAK et al (Minn-ANL)
Estimated normalization uncertainty

Figure 10

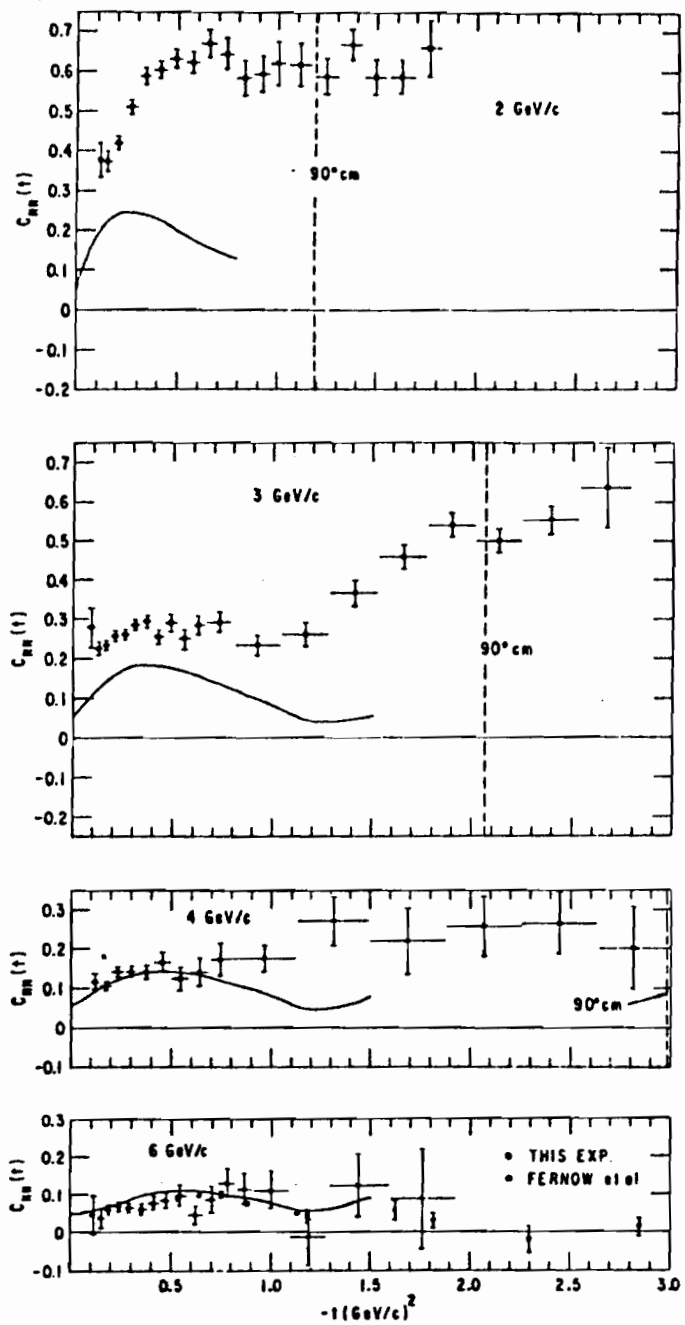
2 GeV/c
90°cm
3 GeV/c
90°cm
4 GeV/c
90°cm
6 GeV/c
• THIS EXP.
• FERNOW et al
$C_{NN}(t)$
$-t\,(GeV/c)^2$

Figure 11A

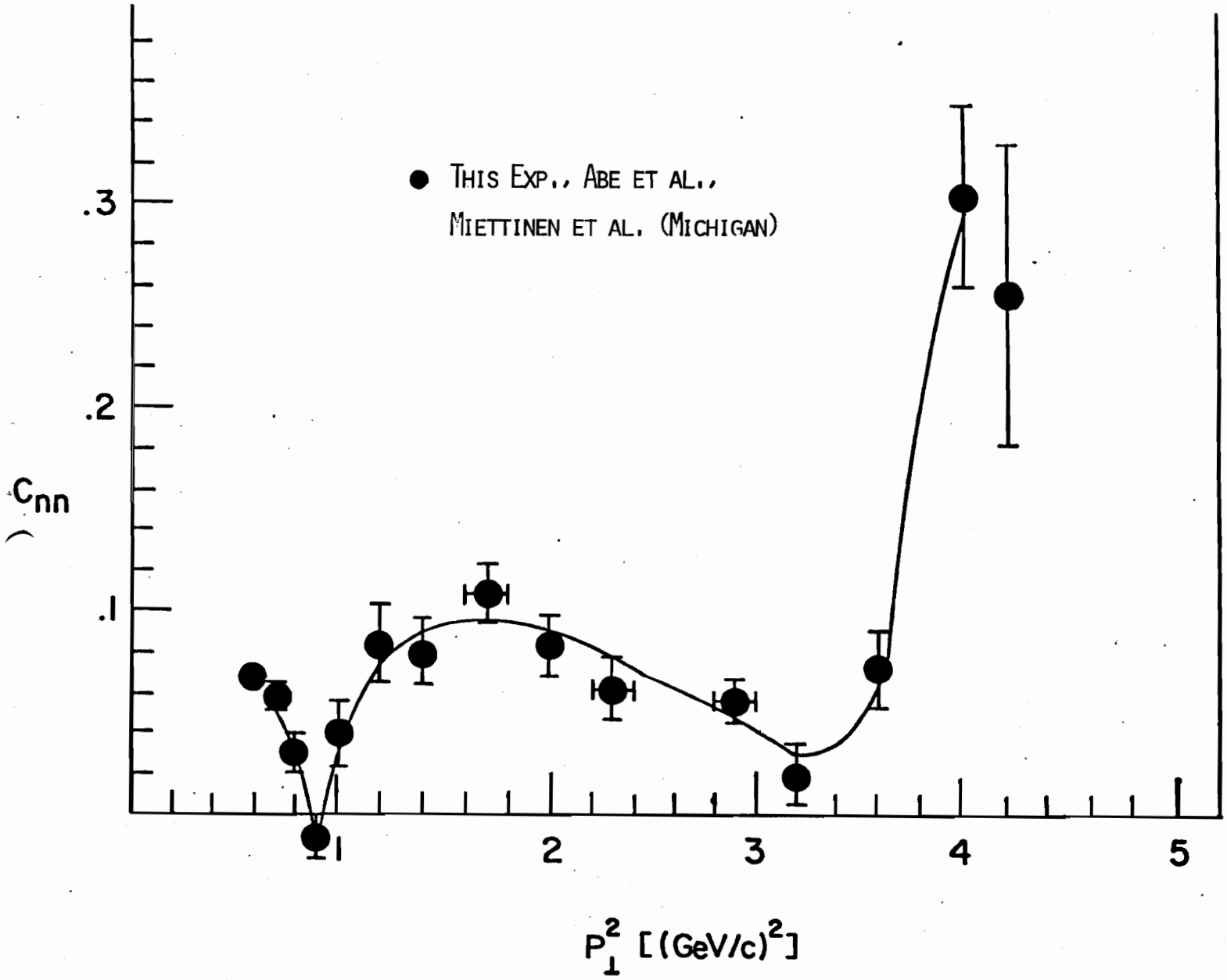
THIS EXP., ABE ET AL.,
MIETTINEN ET AL. (MICHIGAN)
.3
.2
.1
C_{nn}
1
2
3
4
5
$P_\perp^2$ [(GeV/c)^2]

Figure 11B

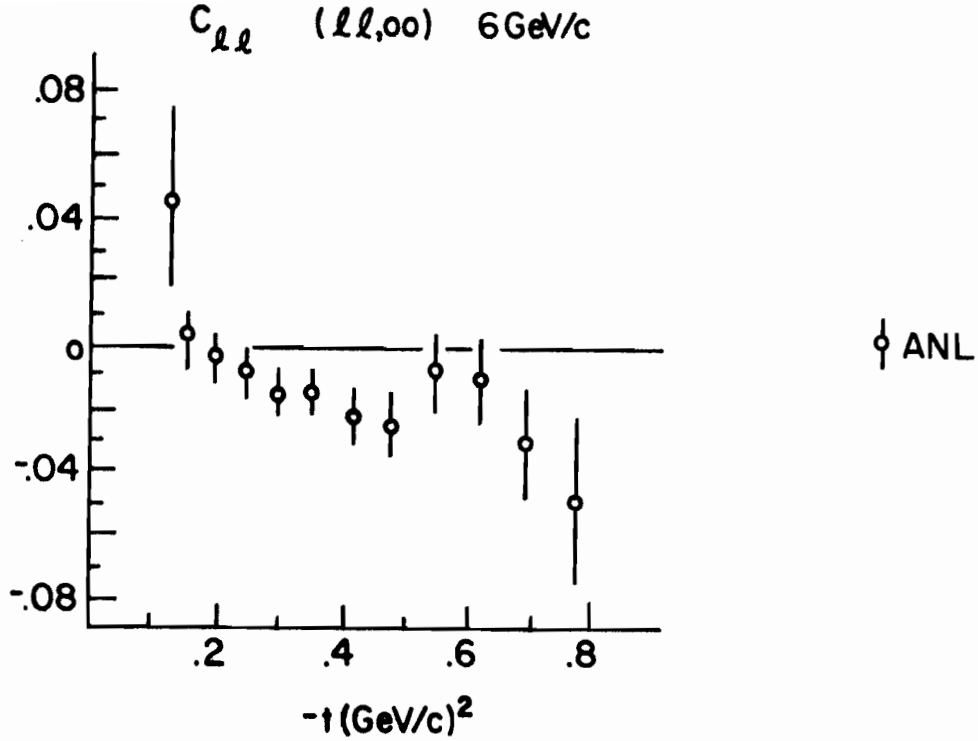
$C_{\ell\ell}$ ($\ell\ell$,oo) 6GeV/c
.08
.04
0
-.04
-.08
.2
.4
.6
.8
-t (GeV/c)^2
ANL

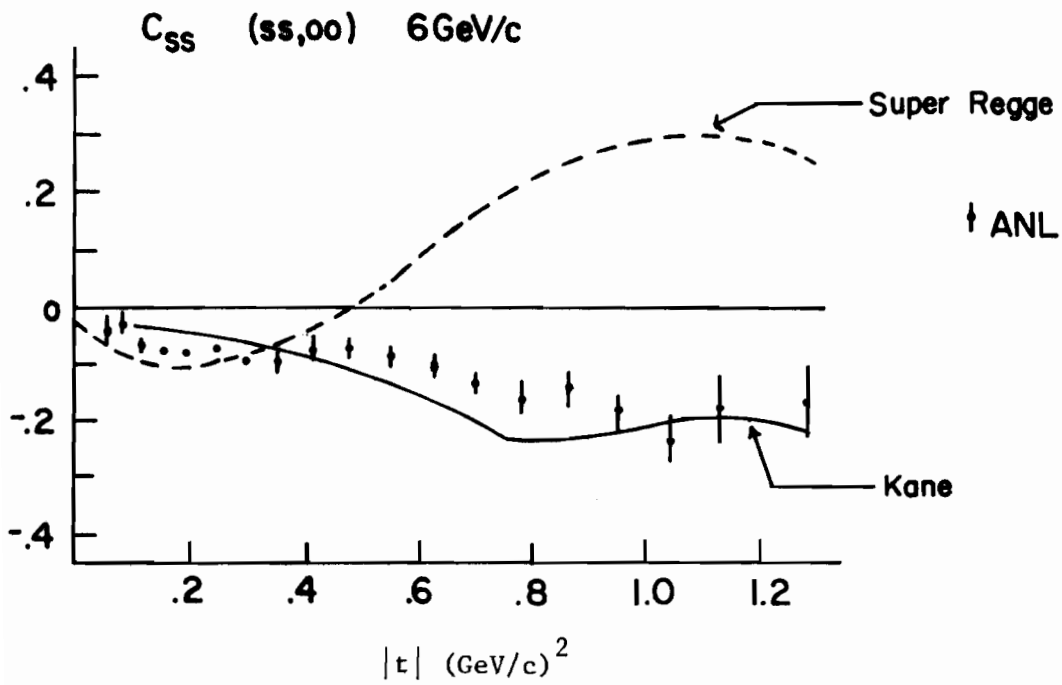
C_{ss} (ss,oo) 6GeV/c
.4
.2
0
-.2
-.4
.2
.4
.6
.8
1.0
1.2
|t| (GeV/c)^2
Super Regge
ANL
Kane

Figure 12

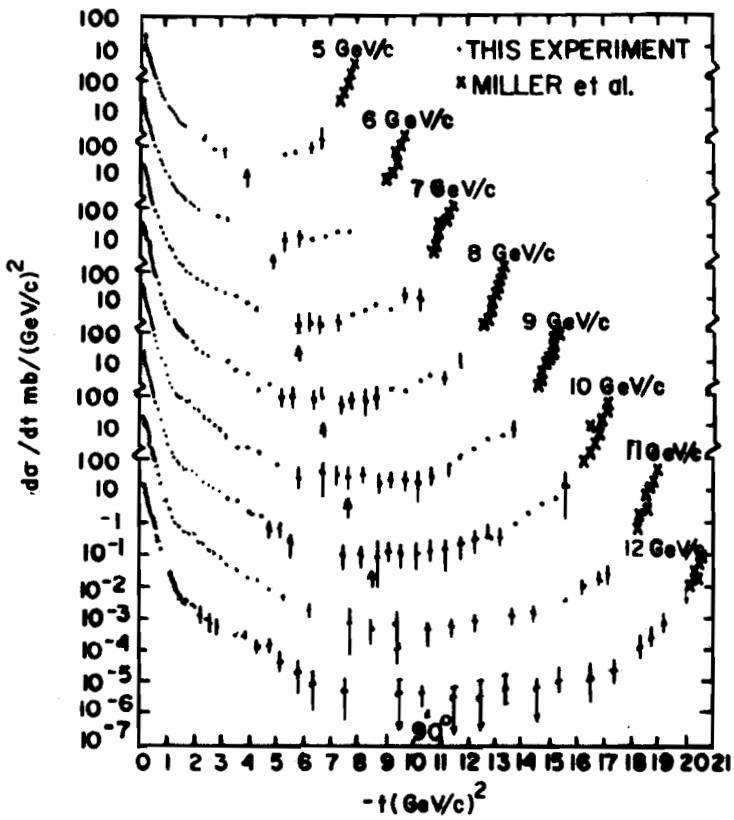
5 GeV/c
6 GeV/c
7 GeV/c
8 GeV/c
9 GeV/c
10 GeV/c
11 GeV/c
12 GeV/c
·THIS EXPERIMENT
×MILLER et al.
90°
dσ/dt mb/(GeV/c)²
-t(GeV/c)²

Figure 13

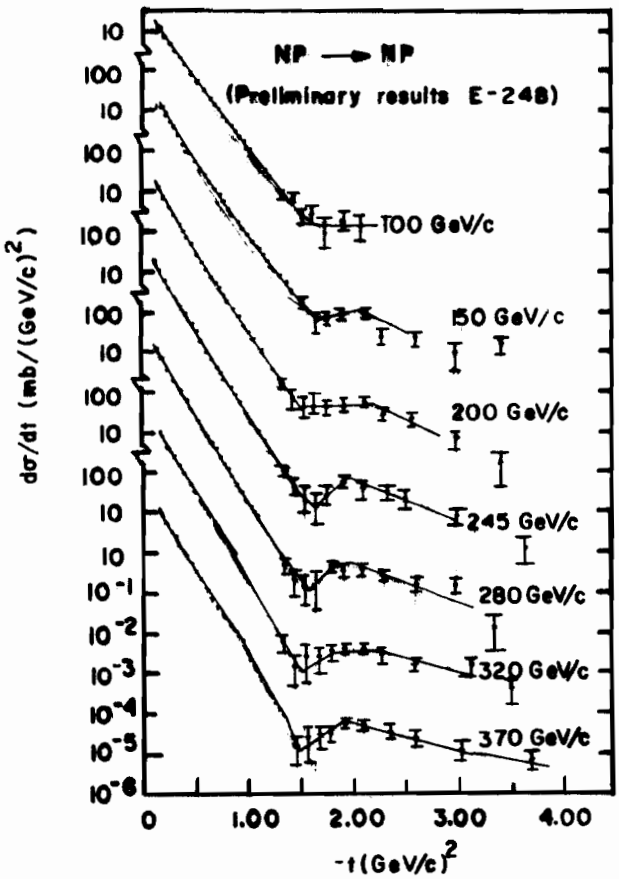
NP → NP
(Preliminary results E-248)
100 GeV/c
150 GeV/c
200 GeV/c
245 GeV/c
280 GeV/c
320 GeV/c
370 GeV/c
dσ/dt (mb/(GeV/c)²)
-t(GeV/c)²
0
1.00
2.00
3.00
4.00

Figure 14

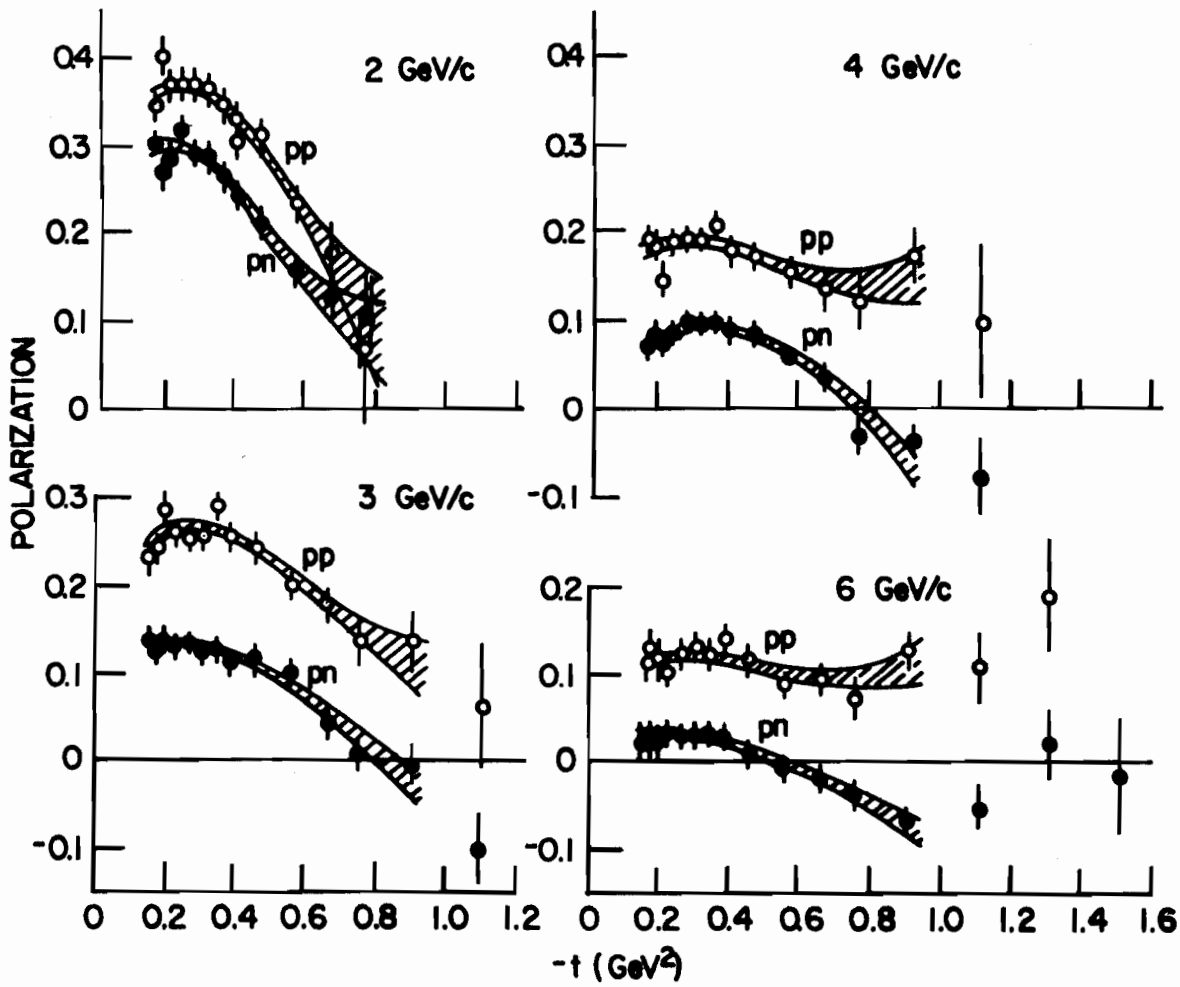
2 GeV/c
4 GeV/c
3 GeV/c
6 GeV/c
pp
pn
POLARIZATION
-t (GeV²)
0.4
0.3
0.2
0.1
0
-0.1
0.2
0.4
0.6
0.8
1.0
1.2
1.4
1.6

Figure 15A

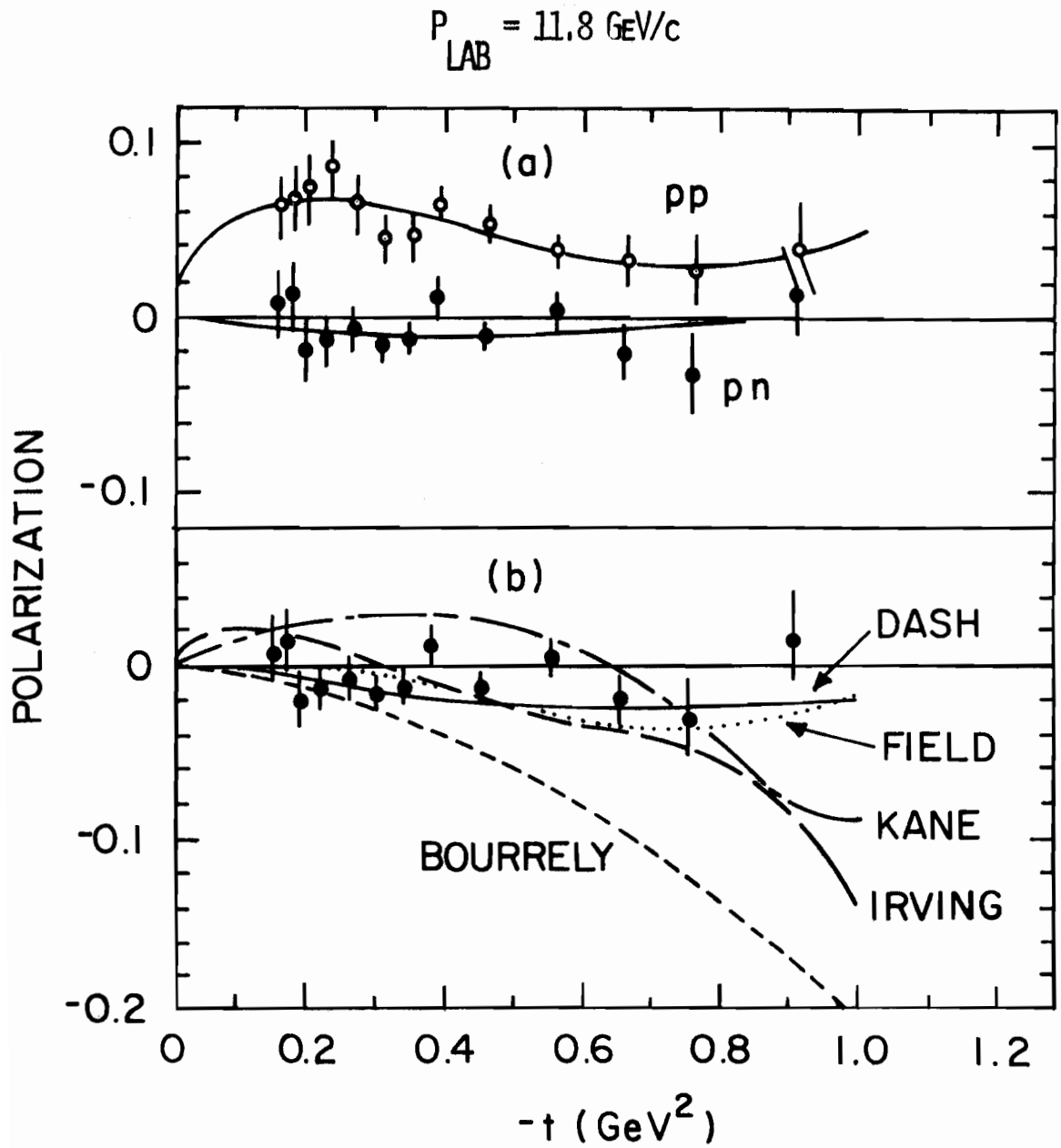
P LAB = 11.8 GeV/c
(a)
pp
pn
(b)
DASH
FIELD
KANE
IRVING
BOURRELY
POLARIZATION
0.1
0
-0.1
-0.2
0
0.2
0.4
0.6
0.8
1.0
1.2
-t (GeV²)

Figure 15B

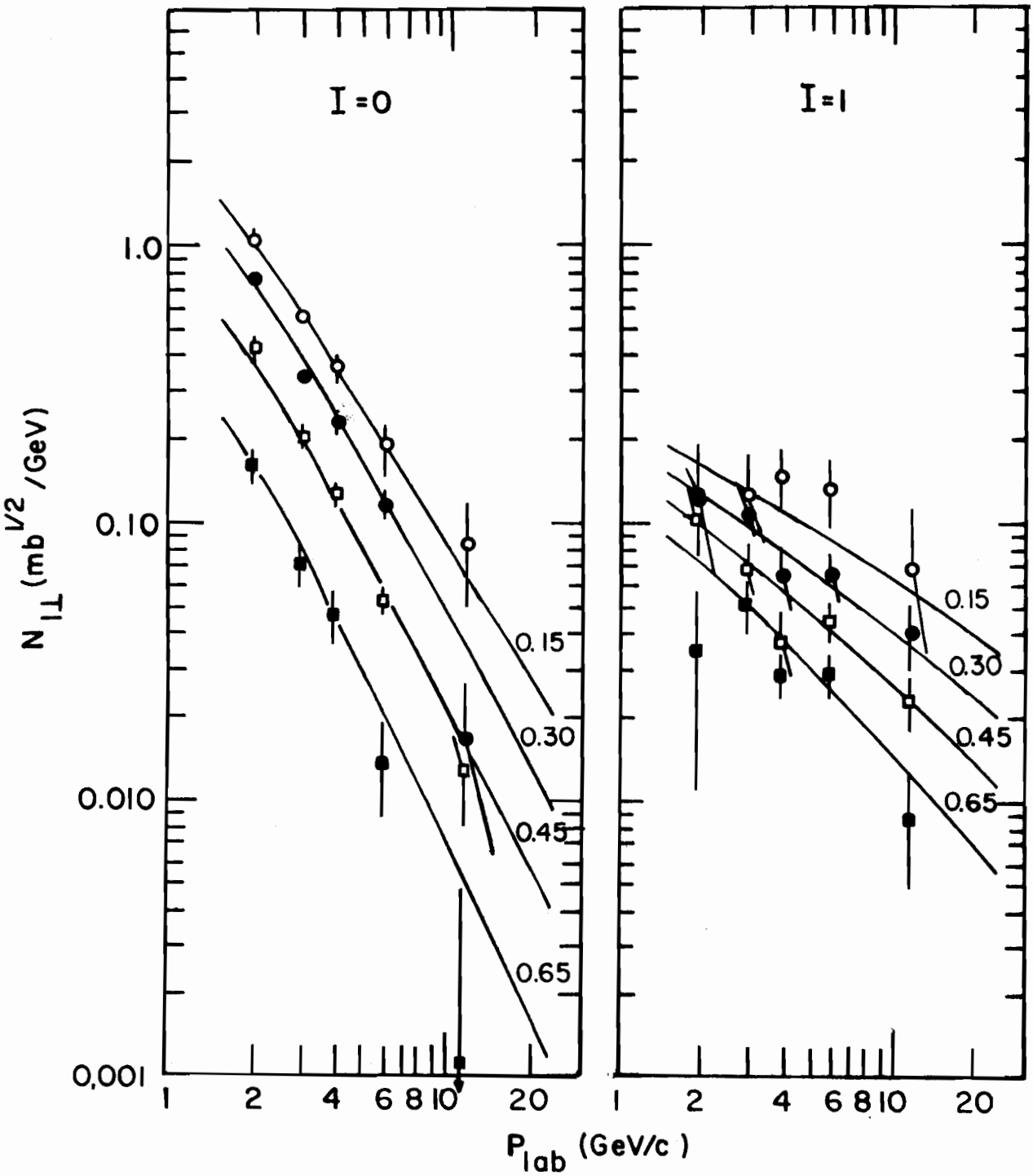
I = 0
I = 1
1.0
0.10
0.010
0.001
$N_{1\perp}$ (mb$^{1/2}$/GeV)
0.15
0.30
0.45
0.65
1
2
4
6
8
10
20
P_{lab} (GeV/c)

Figure 16

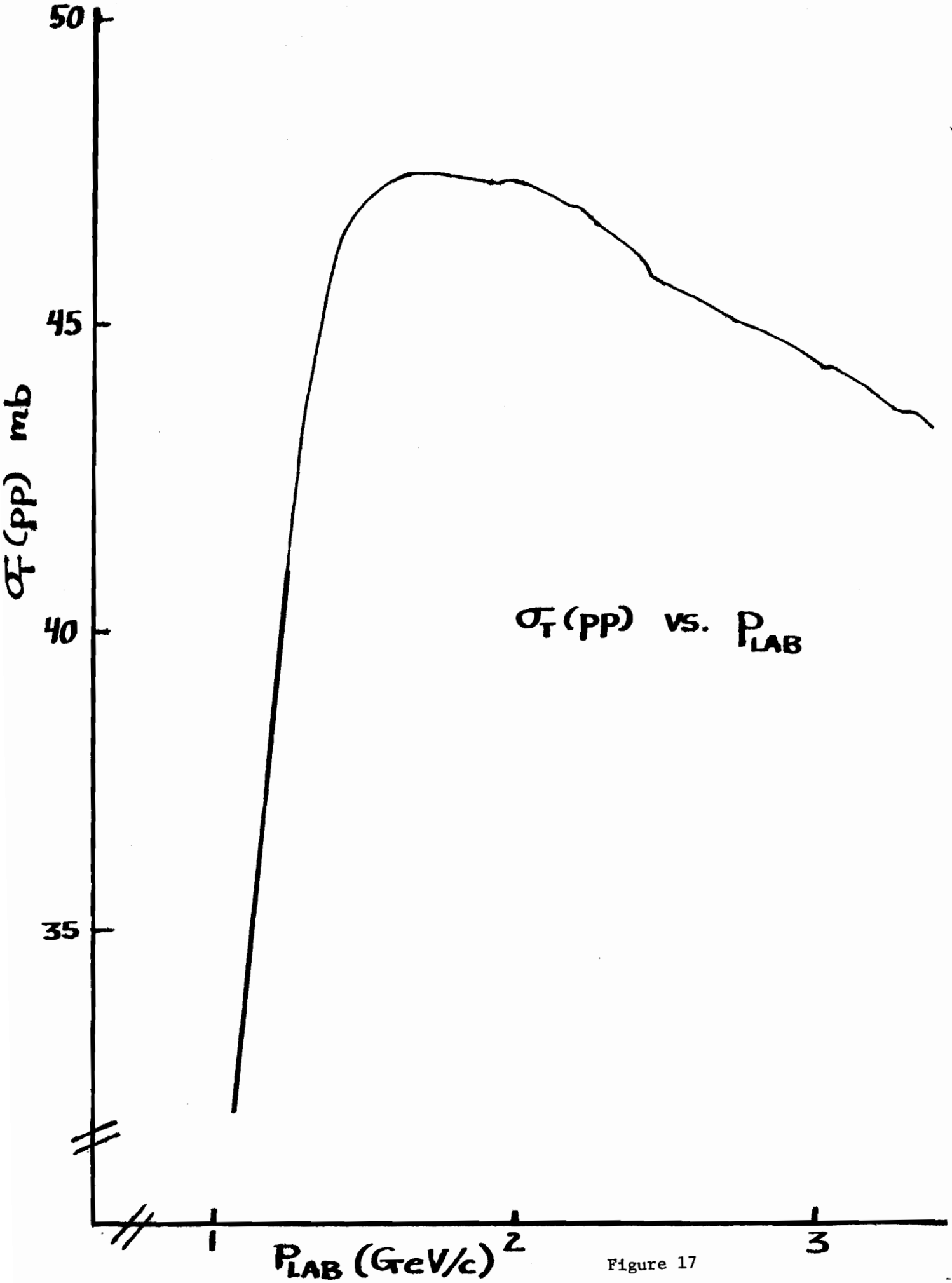

Figure 17

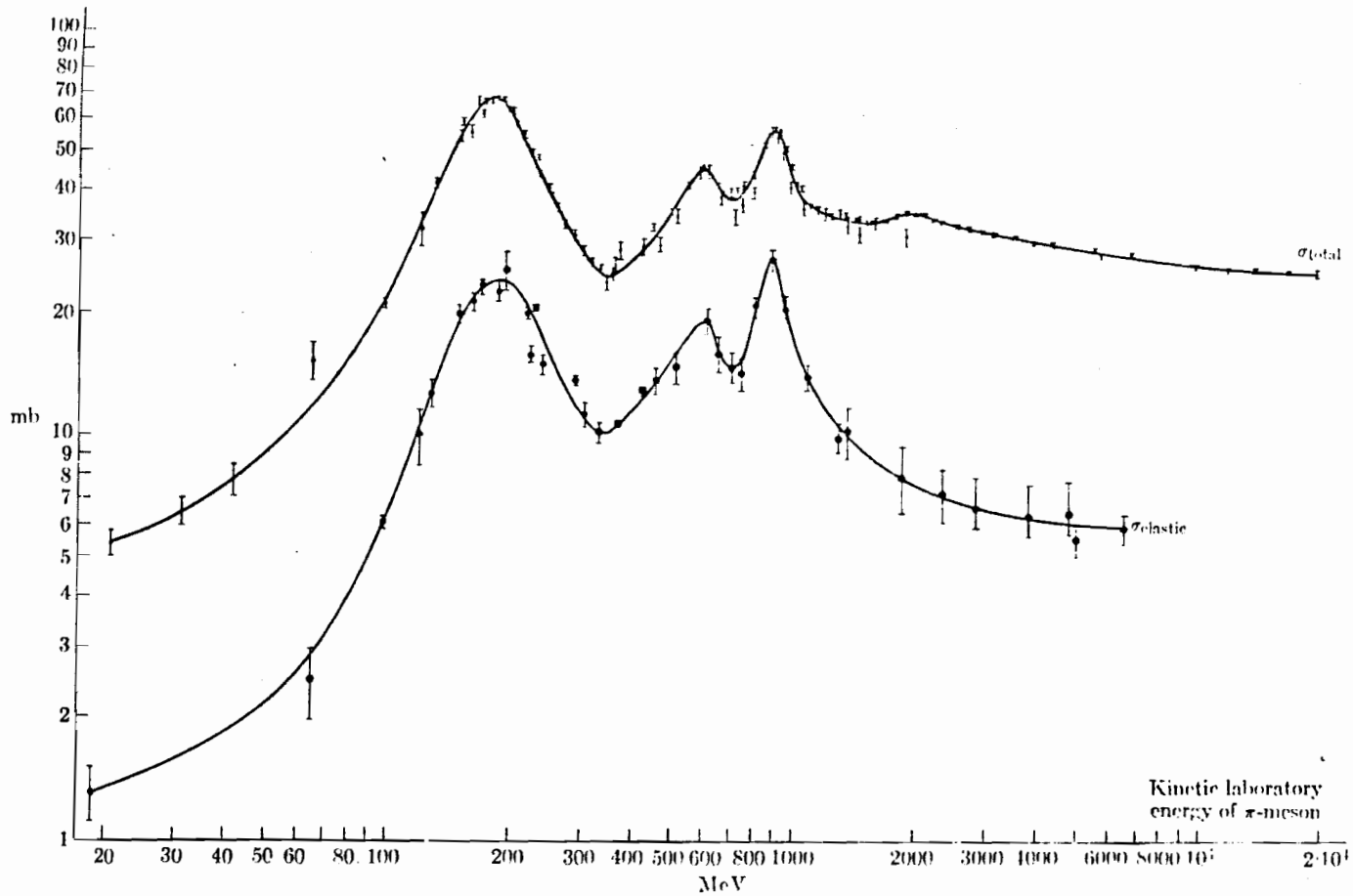
mb
100
90
80
70
60
50
40
30
20
10
9
8
7
6
5
4
3
2
1
σ_{total}
$\sigma_{elastic}$
Kinetic laboratory energy of π-meson
20
30
40
50
60
80
100
200
300
400
500
600
800
1000
2000
3000
4000
6000
8000
10^4
$2 \cdot 10^4$
MeV

Figure 18

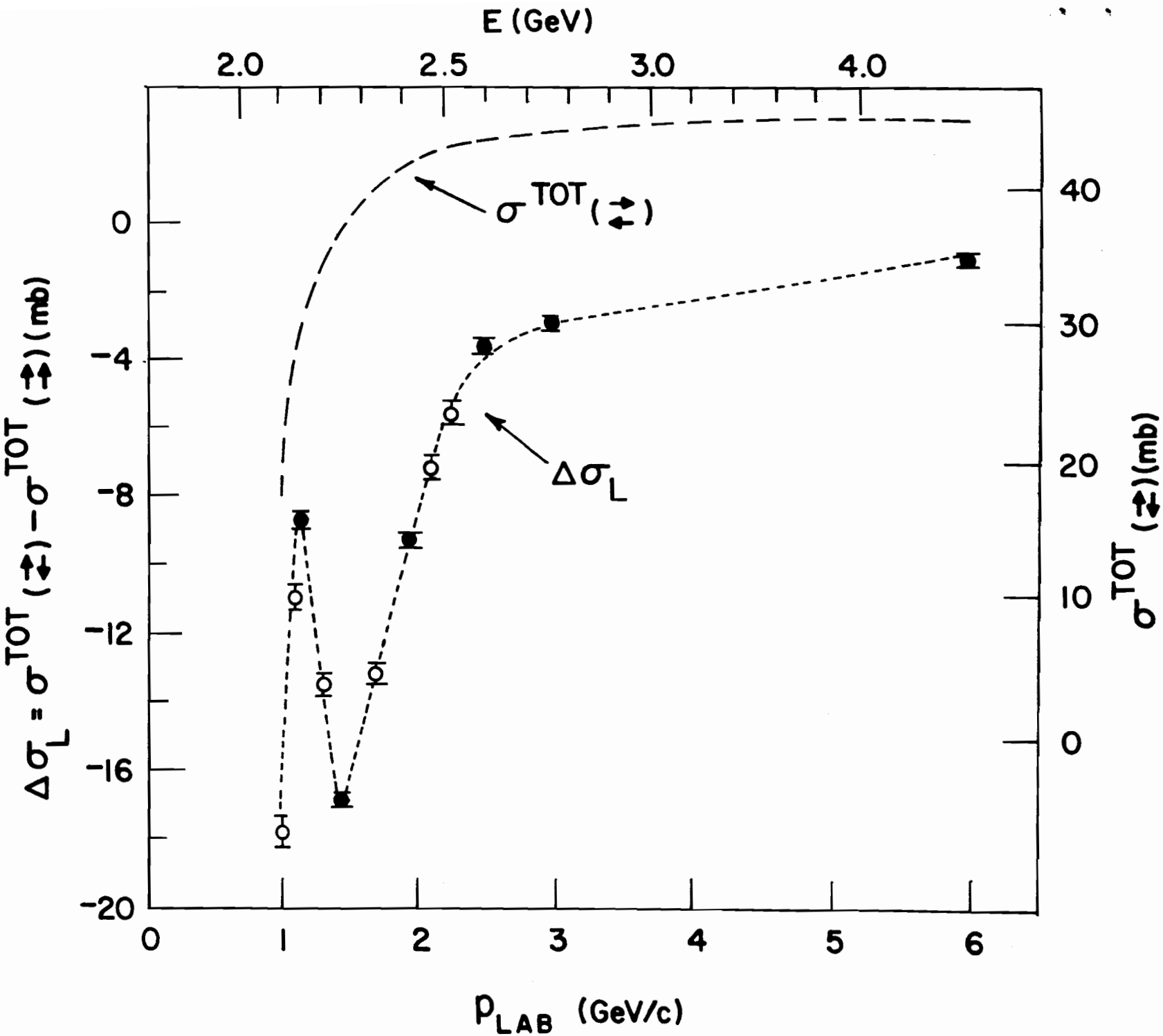
E (GeV)
2.0
2.5
3.0
4.0
$\sigma^{TOT}(\rightleftarrows)$
$\Delta\sigma_L$
$\Delta\sigma_L = \sigma^{TOT}(\uparrow\downarrow) - \sigma^{TOT}(\uparrow\uparrow)$ (mb)
$\sigma^{TOT}(\uparrow\downarrow)$ (mb)
0
-4
-8
-12
-16
-20
40
30
20
10
0
0
1
2
3
4
5
6
p_{LAB} (GeV/c)

Figure 19

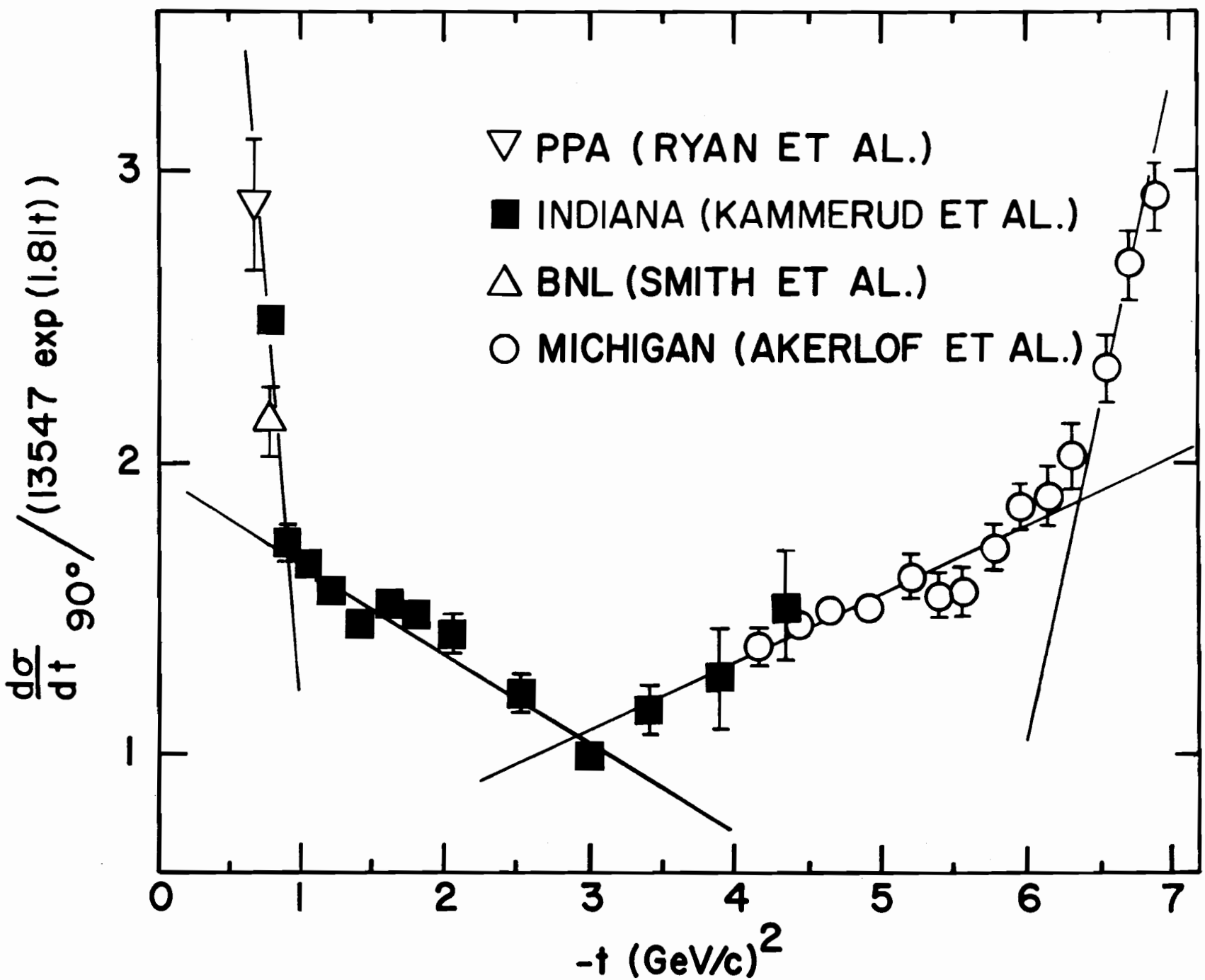
▽ PPA (RYAN ET AL.)
■ INDIANA (KAMMERUD ET AL.)
△ BNL (SMITH ET AL.)
○ MICHIGAN (AKERLOF ET AL.)
$\frac{d\sigma}{dt}_{90°} / (13547 \exp(1.81t))$
$-t\ (GeV/c)^2$
0
1
2
3
4
5
6
7

Figure 20

(a)

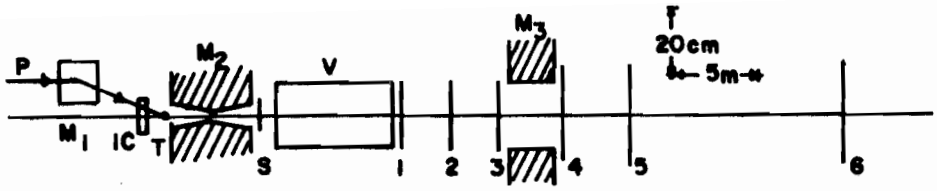

(b)

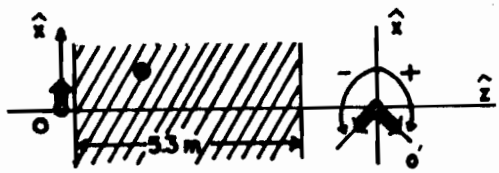

Figure 21

Heller, et al. Phys. Letters 68B, 480, 1977

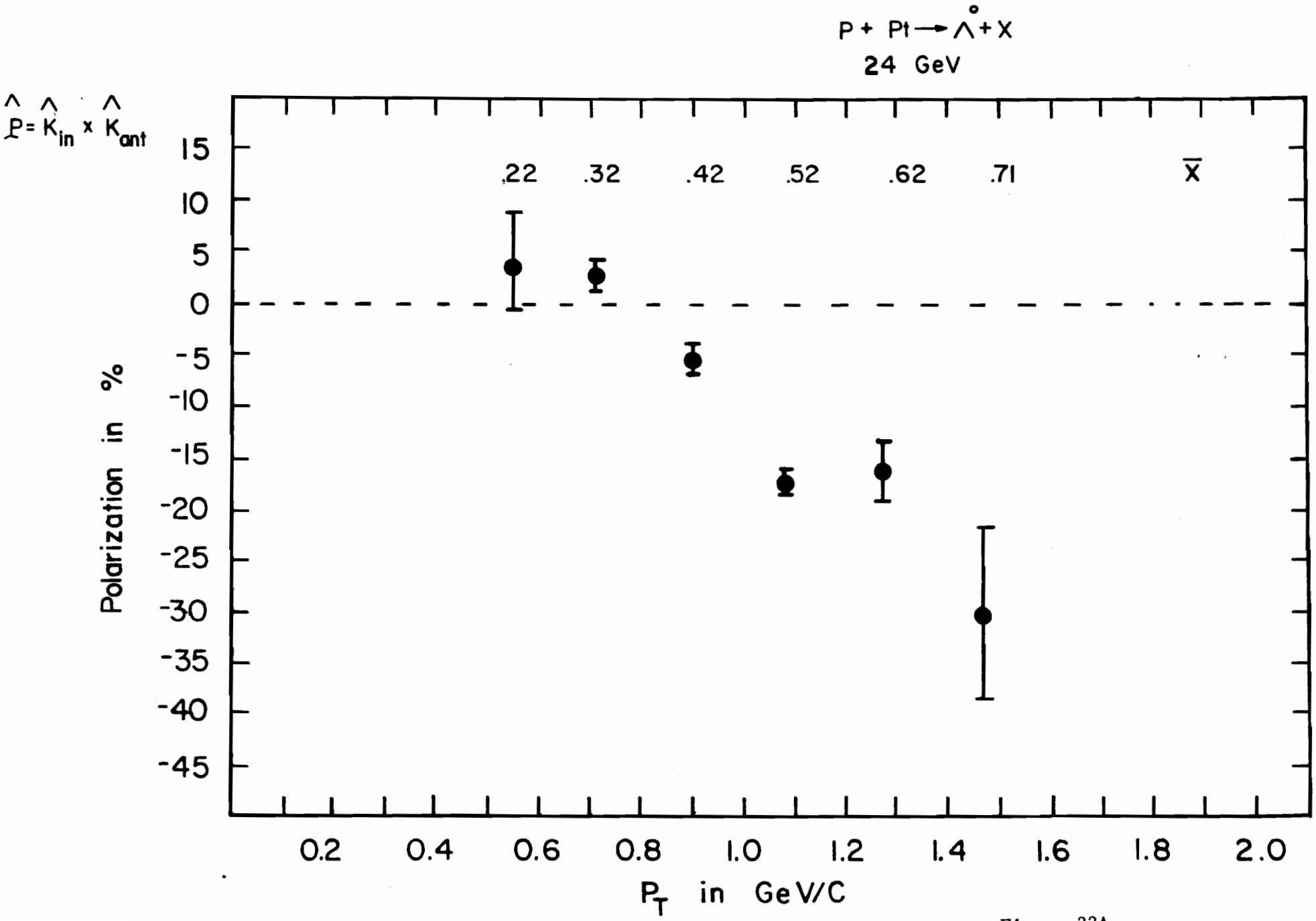

Figure 22A

Bunce, et al. Phys. Rev. Letters 36, 1113, 1976

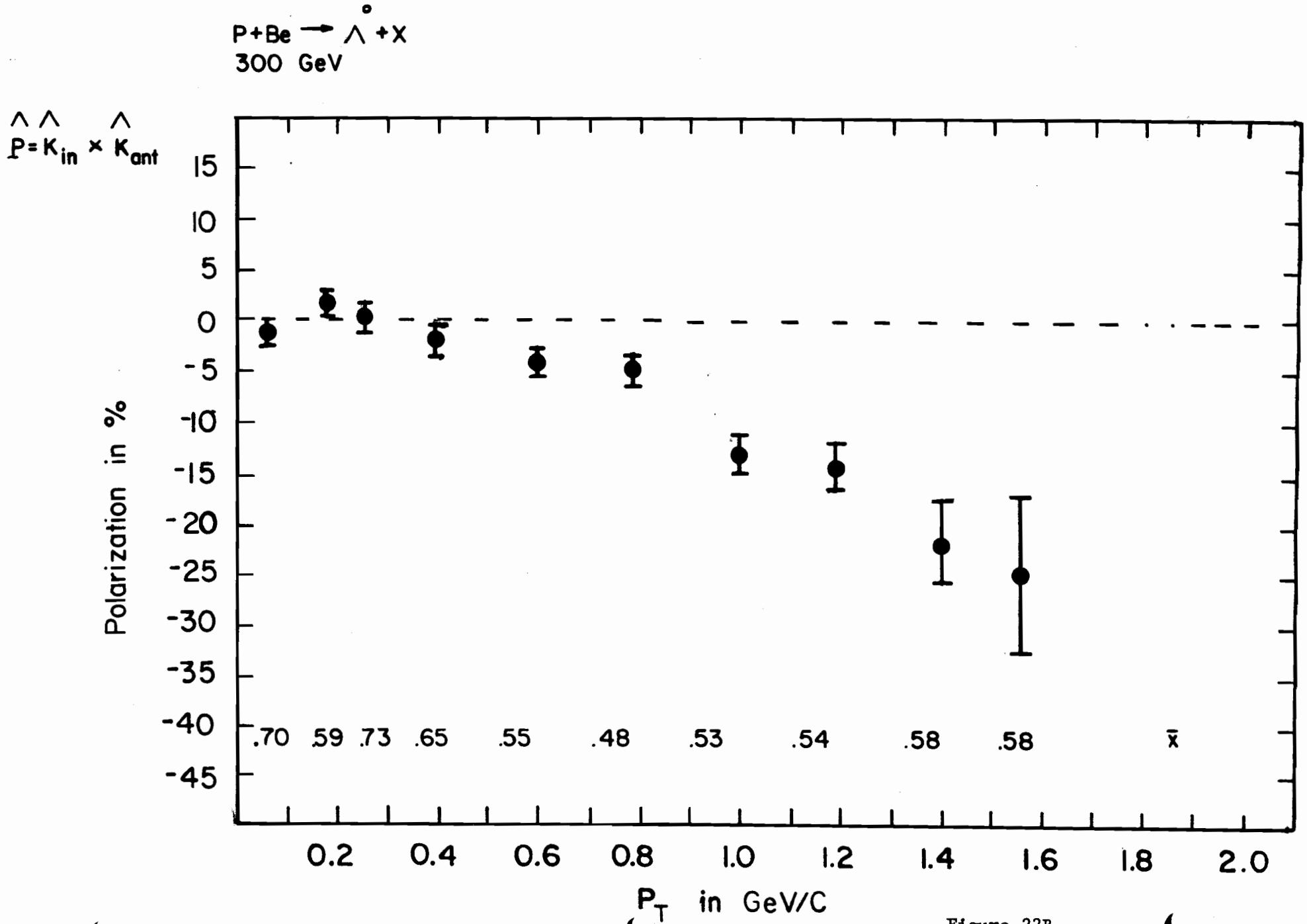

Figure 22B

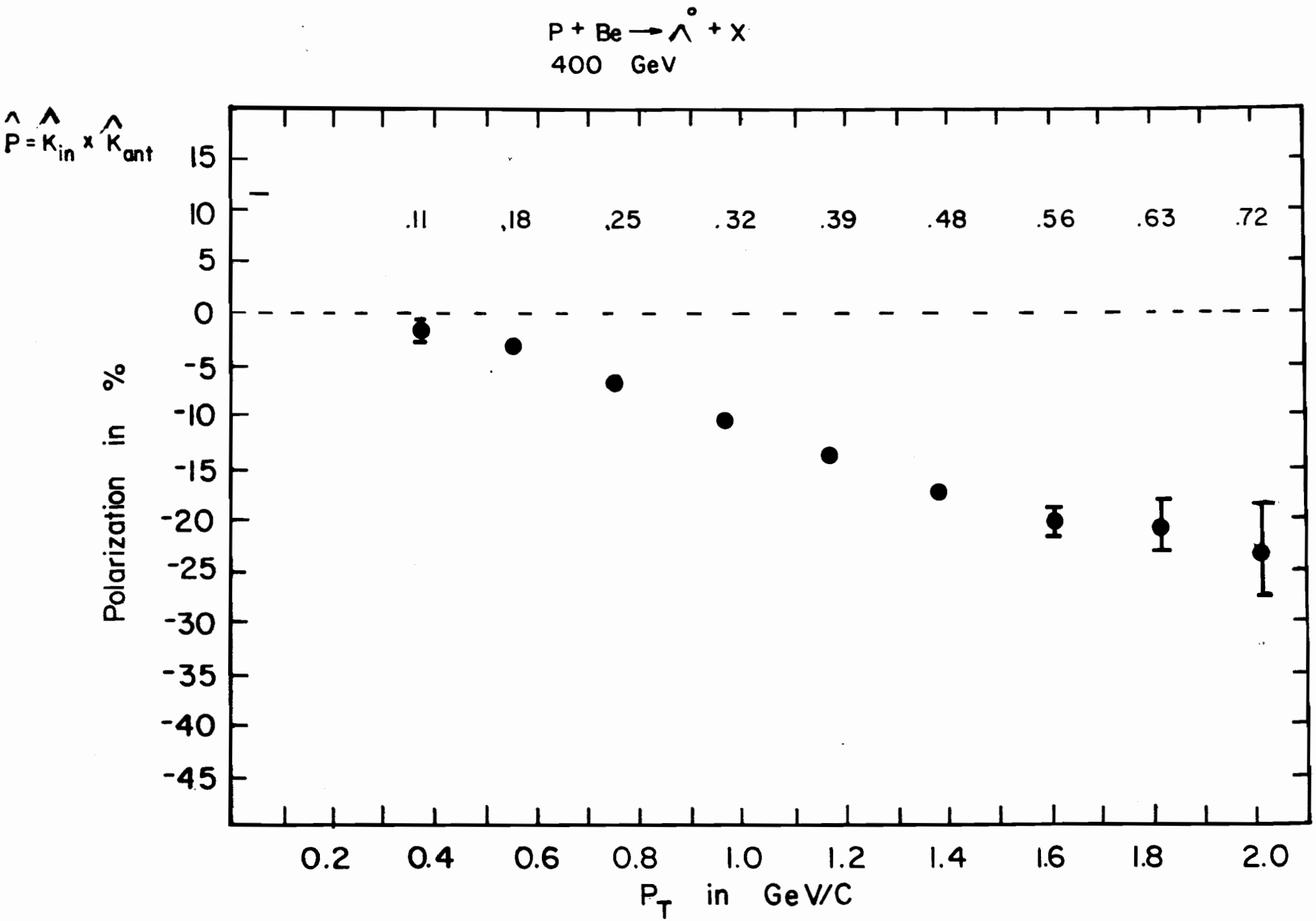
P + Be → Λ° + X
400 GeV
P̂ = K̂in x K̂ant
Polarization in %
15
10
5
0
-5
-10
-15
-20
-25
-30
-35
-40
-45
.11
.18
.25
.32
.39
.48
.56
.63
.72
0.2
0.4
0.6
0.8
1.0
1.2
1.4
1.6
1.8
2.0
PT in GeV/C

Figure 22C

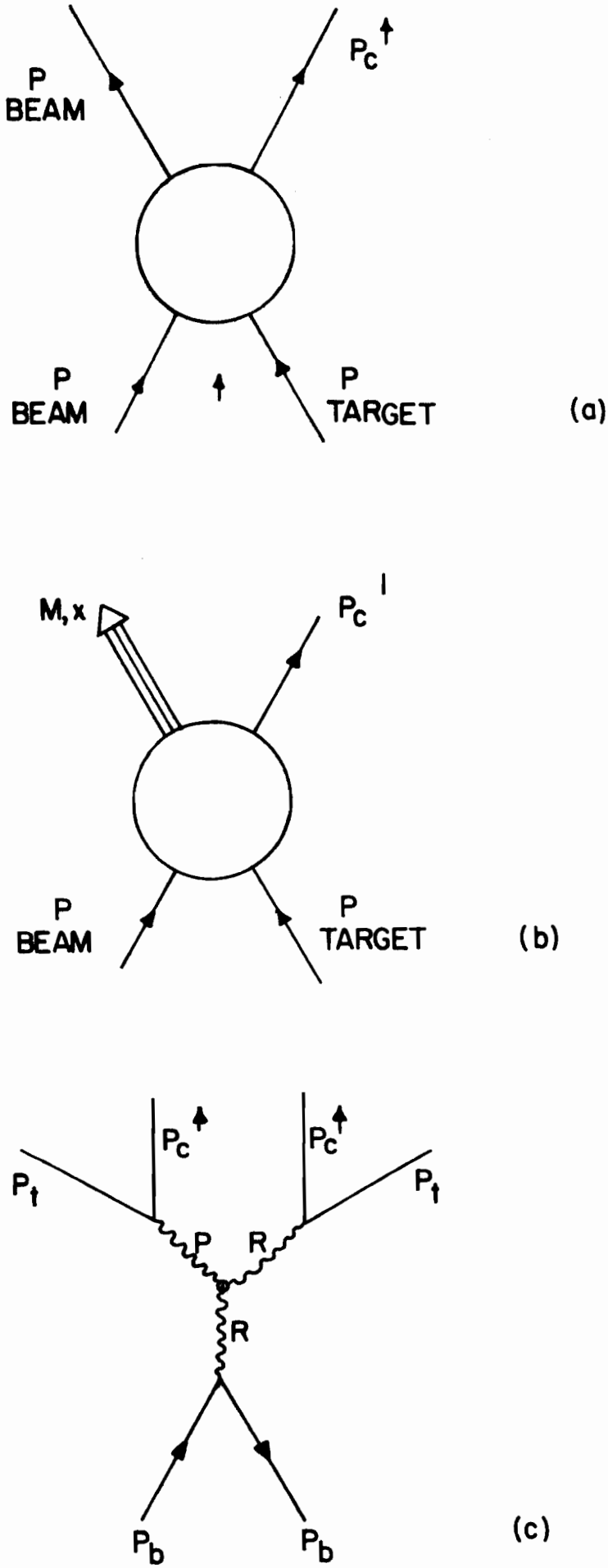
P
BEAM
P_c
P
BEAM
P
TARGET
(a)
M, x
P_c
P
BEAM
P
TARGET
(b)
P_c
P_c
P_t
P_t
P
R
R
P_b
P_b
(c)

Figure 23

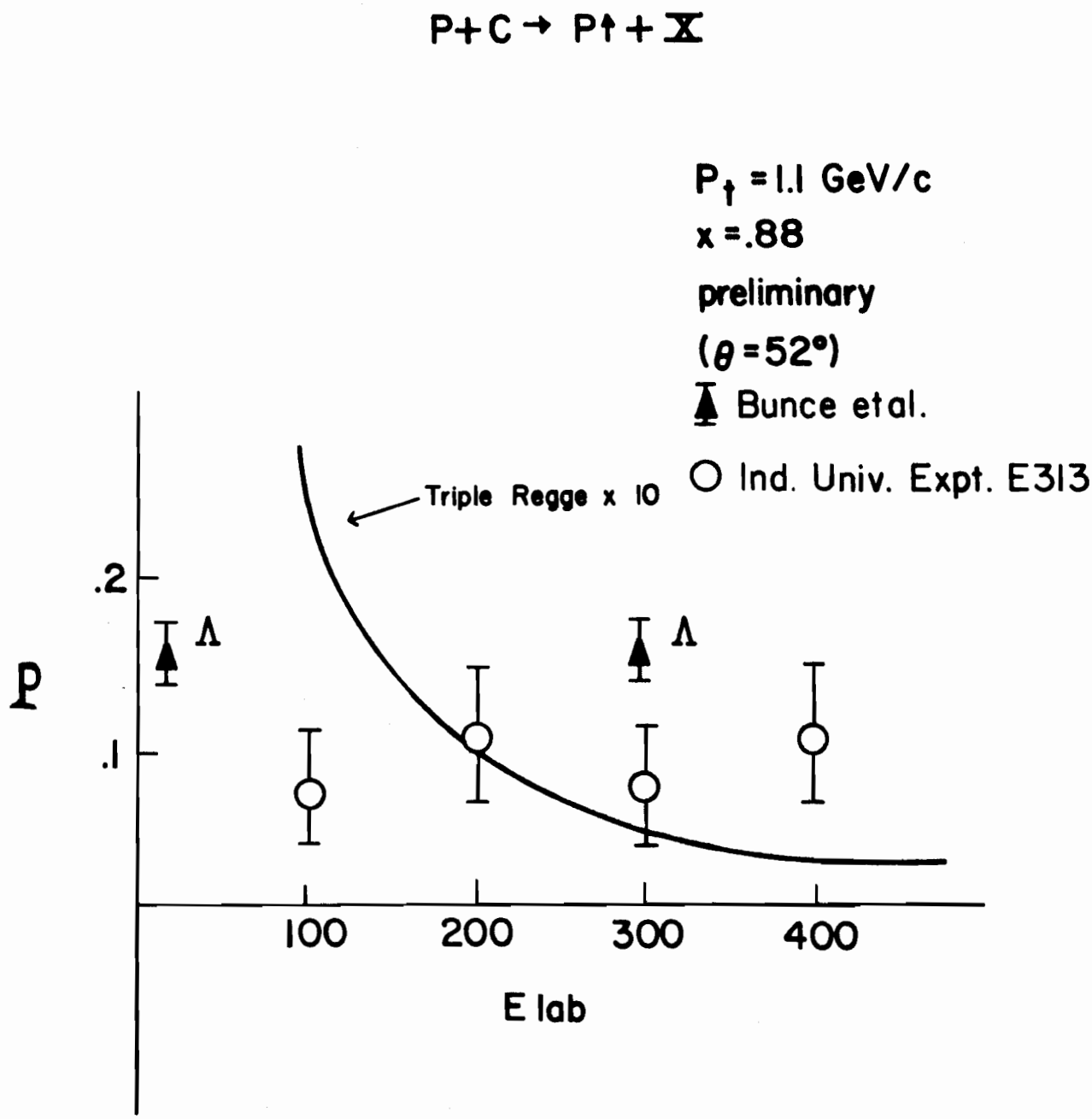
P+C → P↑ + X
P↑ = 1.1 GeV/c
x = .88
preliminary
(θ = 52°)
Bunce et al.
Ind. Univ. Expt. E313
Triple Regge x 10
.2
.1
P
Λ
Λ
100
200
300
400
E lab

Figure 24

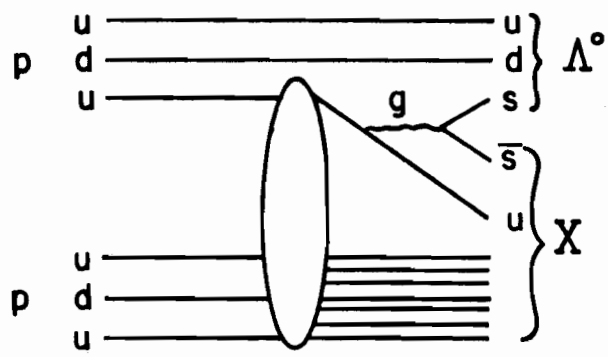

Figure 25

BARYON POLARIZATION

Reaction	Polarization	Ratio of Polarization to Lambda Polarization
$p+p \rightarrow \Lambda^{\circ} + X$	1	1
$p+p \rightarrow p+X$	$\dfrac{3[(u_i,u_i)+(d_i,d_i)]^2 + [3(u_i,u_j)-(d_i,d_j)]^2}{5[(u_i,u_i)+(d_i,d_i)]^2 + [3(u_i,u_j)-(d_i,d_j)]^2}$	$\frac{2}{3}$
$p+p \rightarrow n+X$	$\dfrac{8(d_i,u_i)^2 + 9(d_i,u_j)^2}{10(d_i,u_i)^2 + 9(d_i,u_j)^2}$	$\frac{17}{19}$
$p+p \rightarrow \Sigma^{\circ} + X$	$\dfrac{-3(s_i,u_i)^2 + (s_i,u_j)^2}{5(s_i,u_i)^2 + (s_i,u_j)^2}$	$\frac{-1}{3}$
$p+p \rightarrow \Sigma^{+} + X$	$\dfrac{(s_i,d_j)^2}{2(s_i,d_i)^2 + (s_i,d_j)^2}$	$\frac{1}{3}$
$p+p \rightarrow$ antibaryon $+X$	0	0

Figure 26

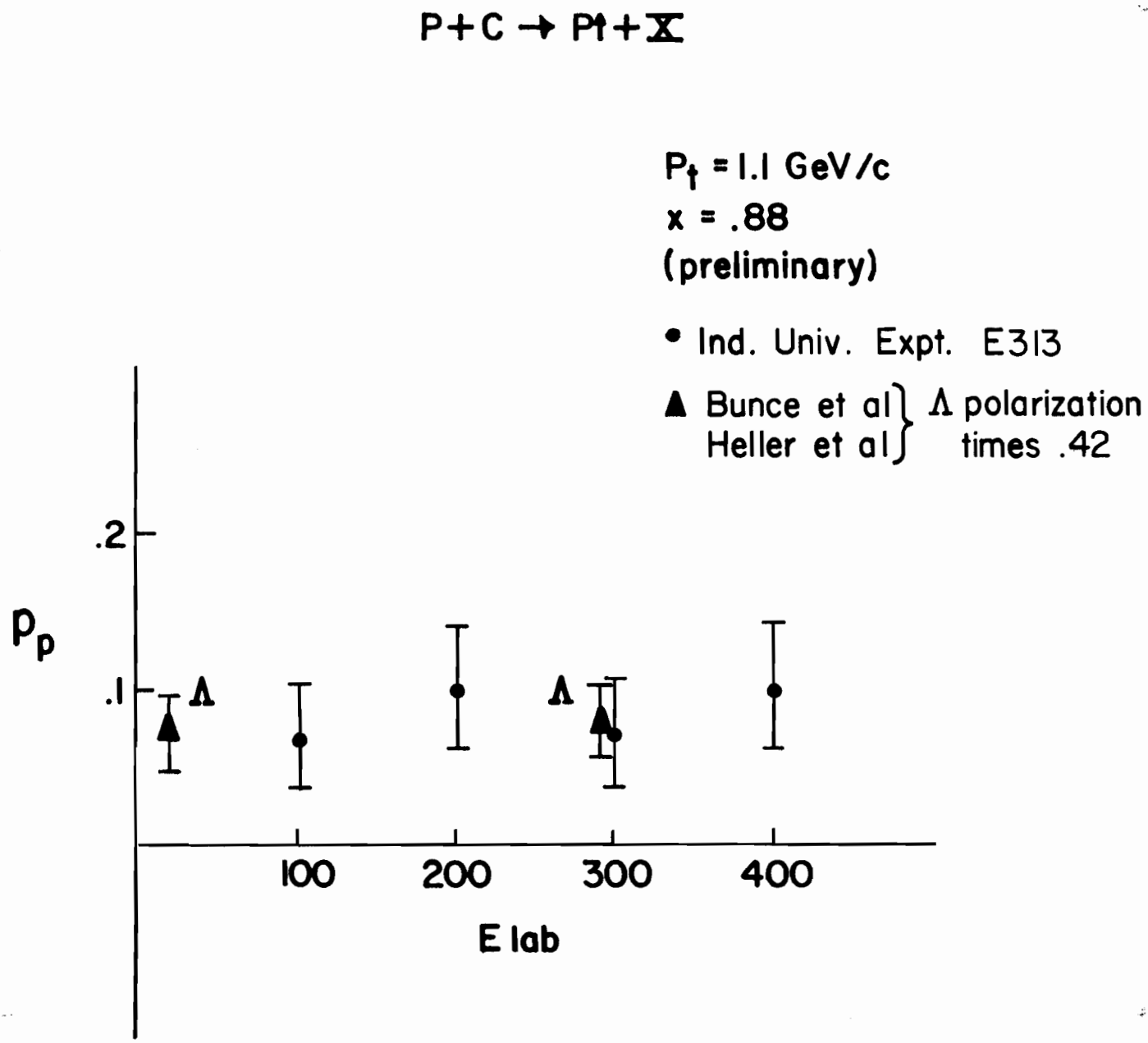
P+C → P↑+X
P_t = 1.1 GeV/c
x = .88
(preliminary)
• Ind. Univ. Expt. E313
▲ Bunce et al
Heller et al
Λ polarization times .42
.2
.1
P_p
Λ
Λ
100
200
300
400
E lab

Figure 27

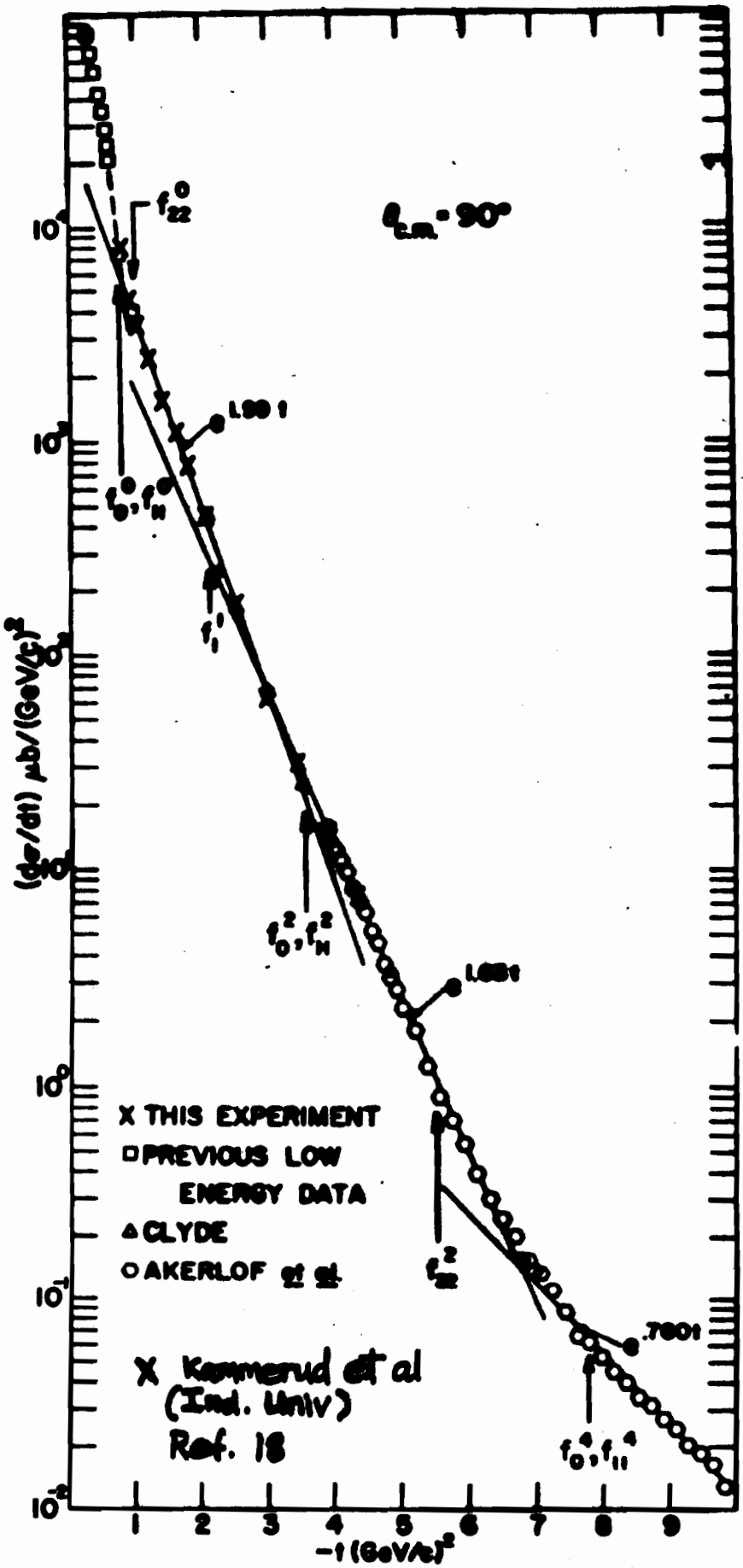
$\theta_{c.m.} = 90°$
f_{22}^0
f_0^0, f_N^0
f_1^1
f_0^2, f_N^2
f_{22}^2
f_0^4, f_{11}^4
1.99 1
1.68 1
.780 1
X THIS EXPERIMENT
□ PREVIOUS LOW ENERGY DATA
△ CLYDE
○ AKERLOF et al.
X Kemmerud et al (Ind. Univ) Ref. 18
$(d\sigma/dt)$ μb/(GeV/c)^2
$-t$ (GeV/c)^2

Figure 28

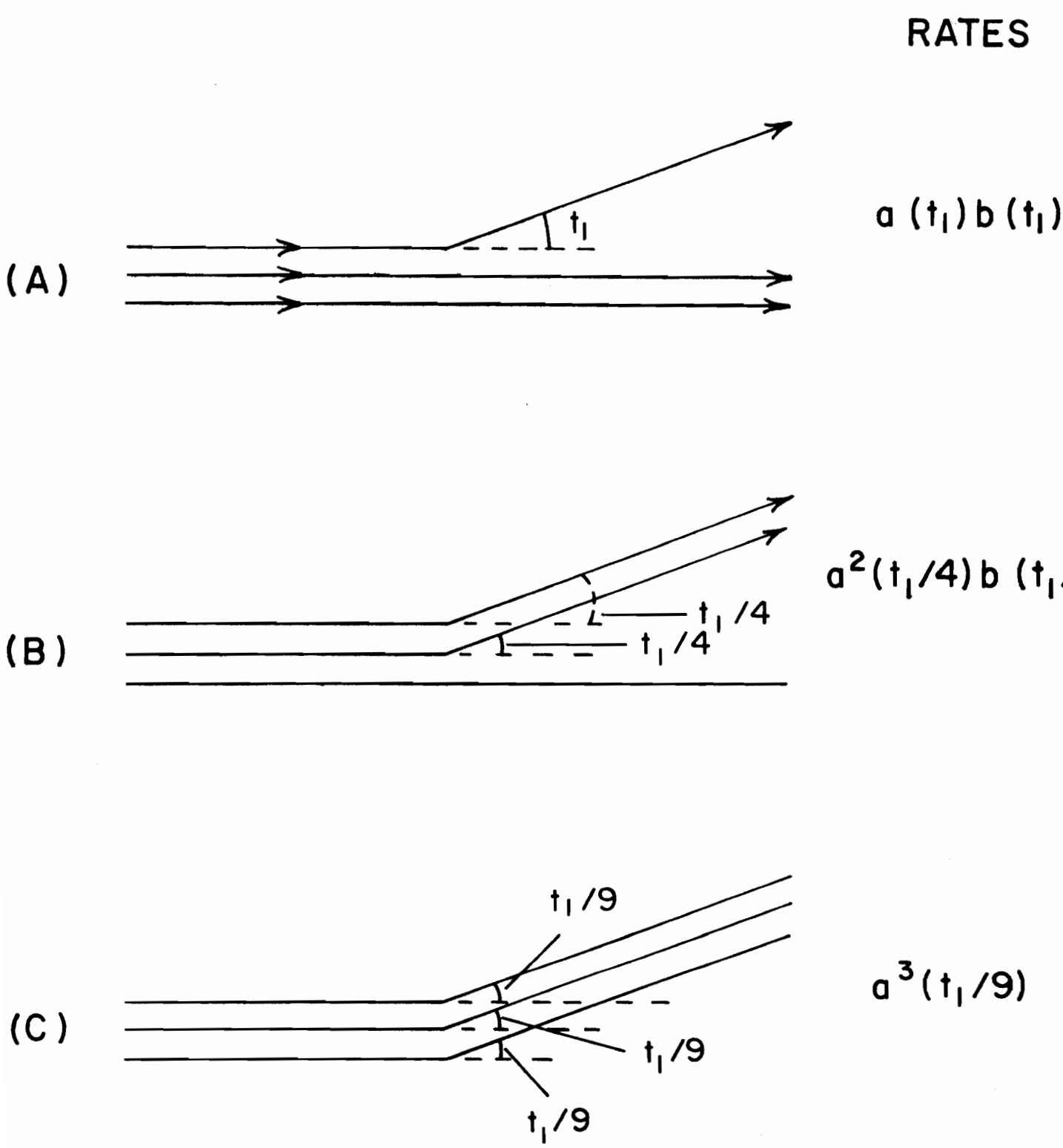

Figure 29

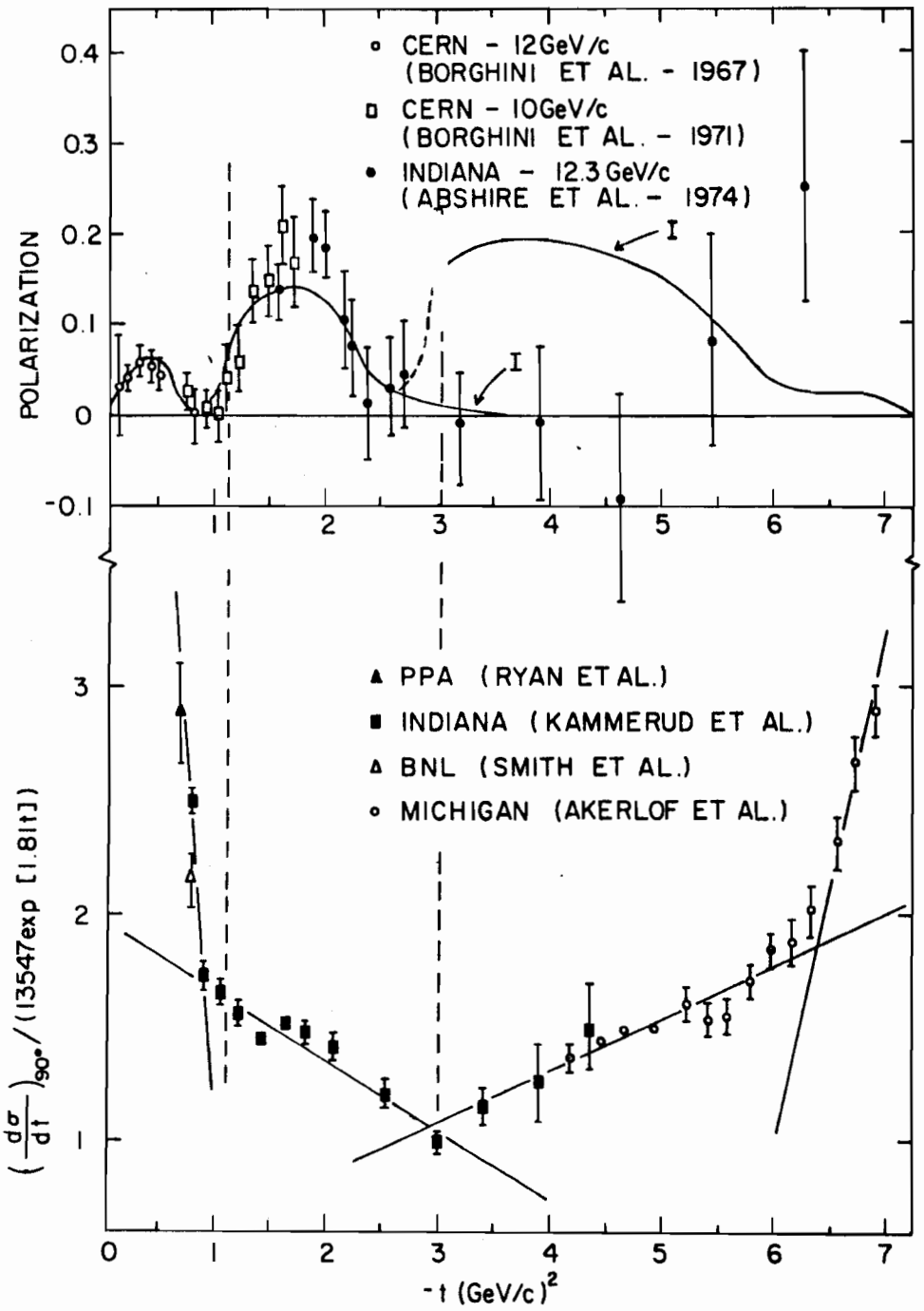
CERN - 12GeV/c
(BORGHINI ET AL. - 1967)
CERN - 10GeV/c
(BORGHINI ET AL. - 1971)
INDIANA - 12.3 GeV/c
(ABSHIRE ET AL. - 1974)
POLARIZATION
PPA (RYAN ET AL.)
INDIANA (KAMMERUD ET AL.)
BNL (SMITH ET AL.)
MICHIGAN (AKERLOF ET AL.)
$\left(\frac{d\sigma}{dt}\right)_{90°} / (13547 \exp[1.81t])$
$-t\ (GeV/c)^2$

Figure 30

6 GeV/c, $|t| \approx 0.3$

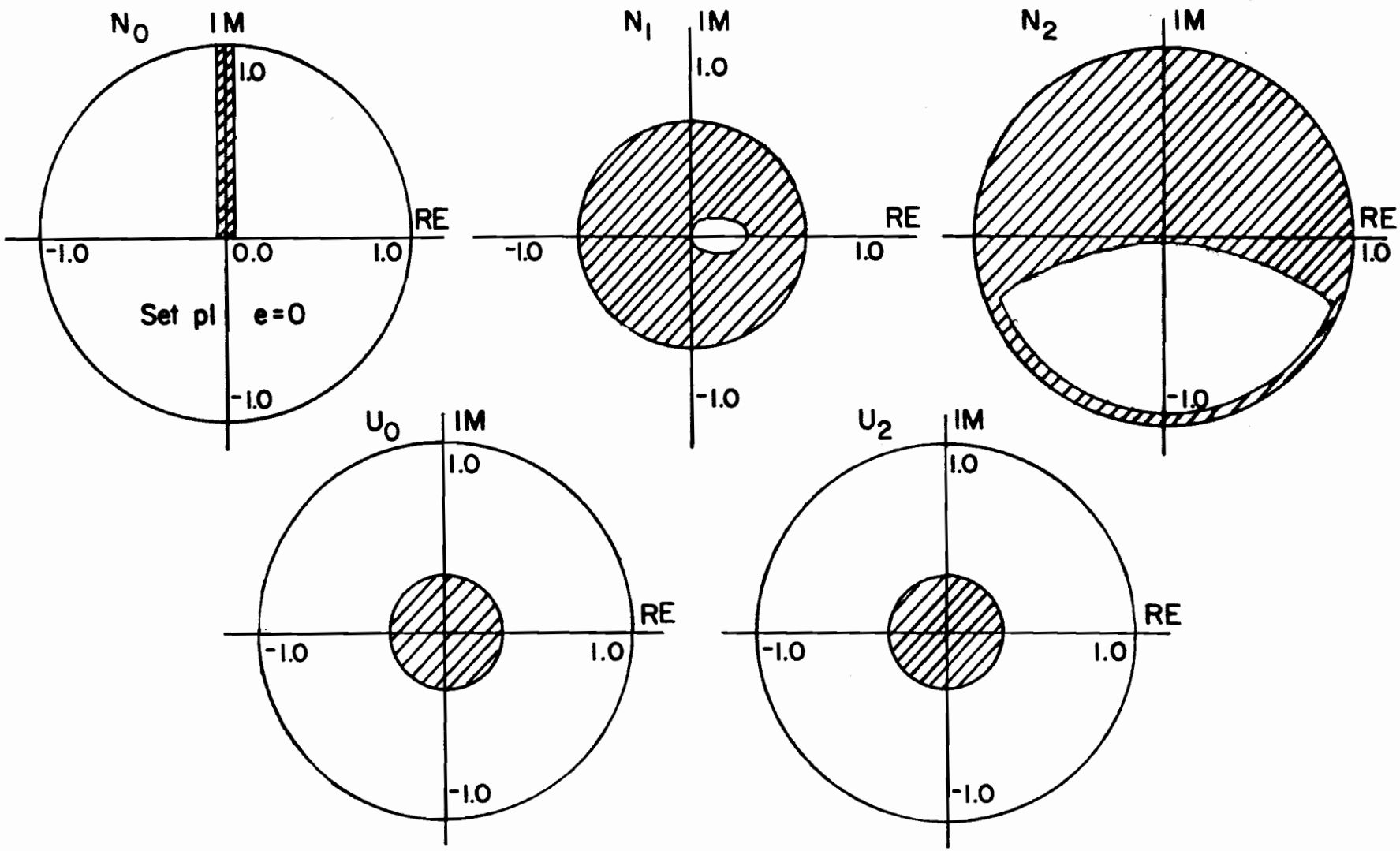

Figure 31A

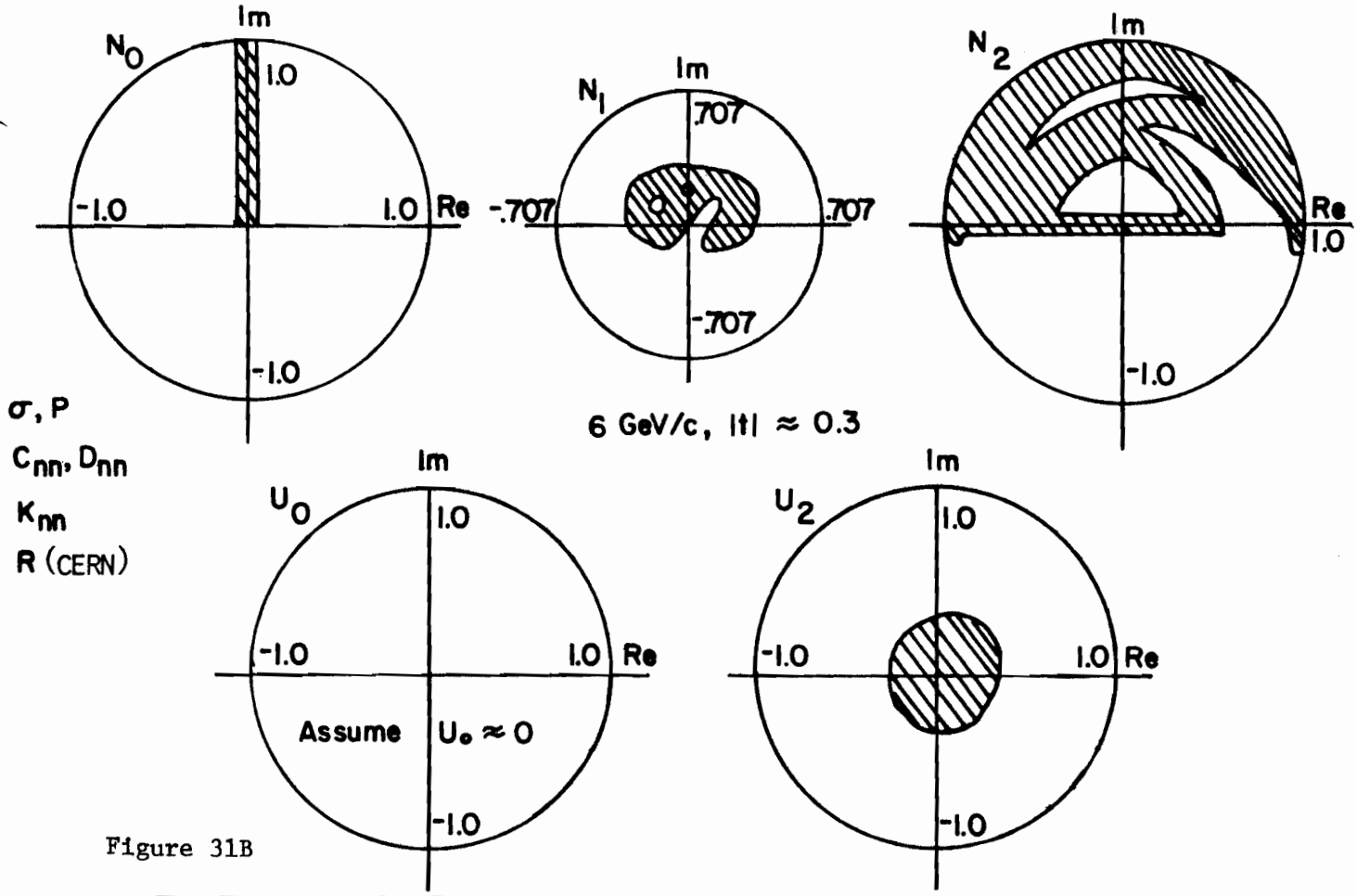

Figure 31B

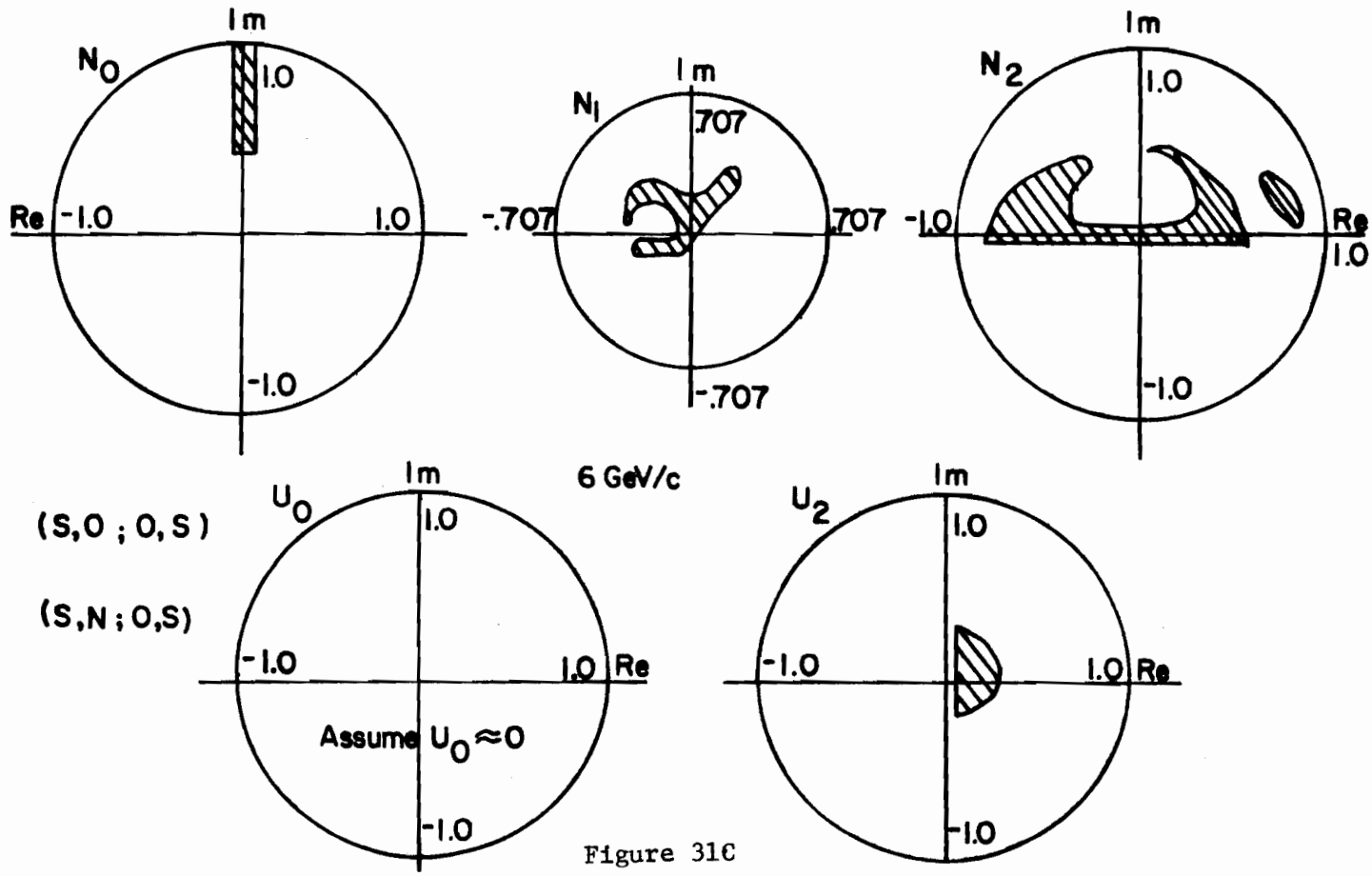

Figure 31C

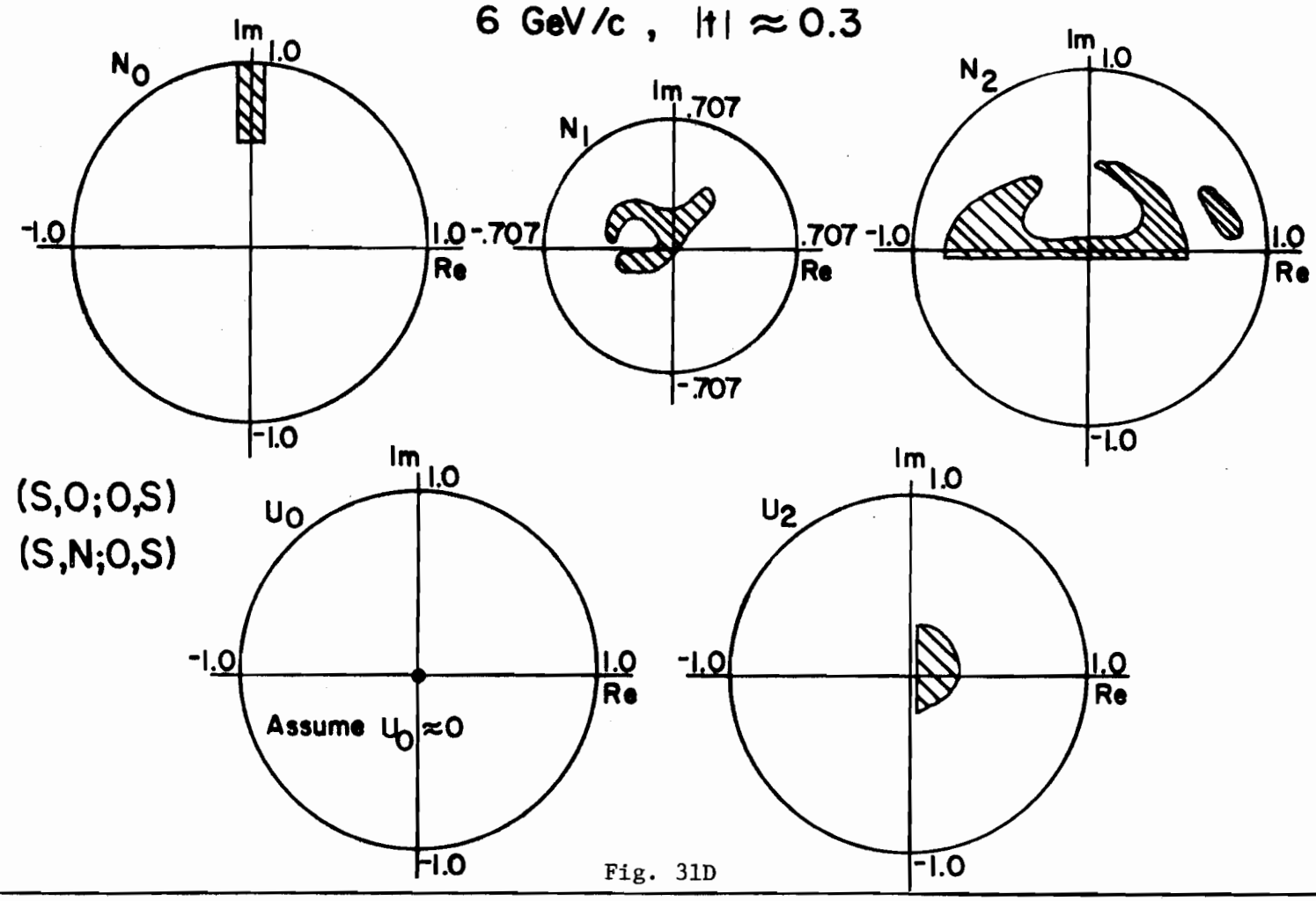

Fig. 31D

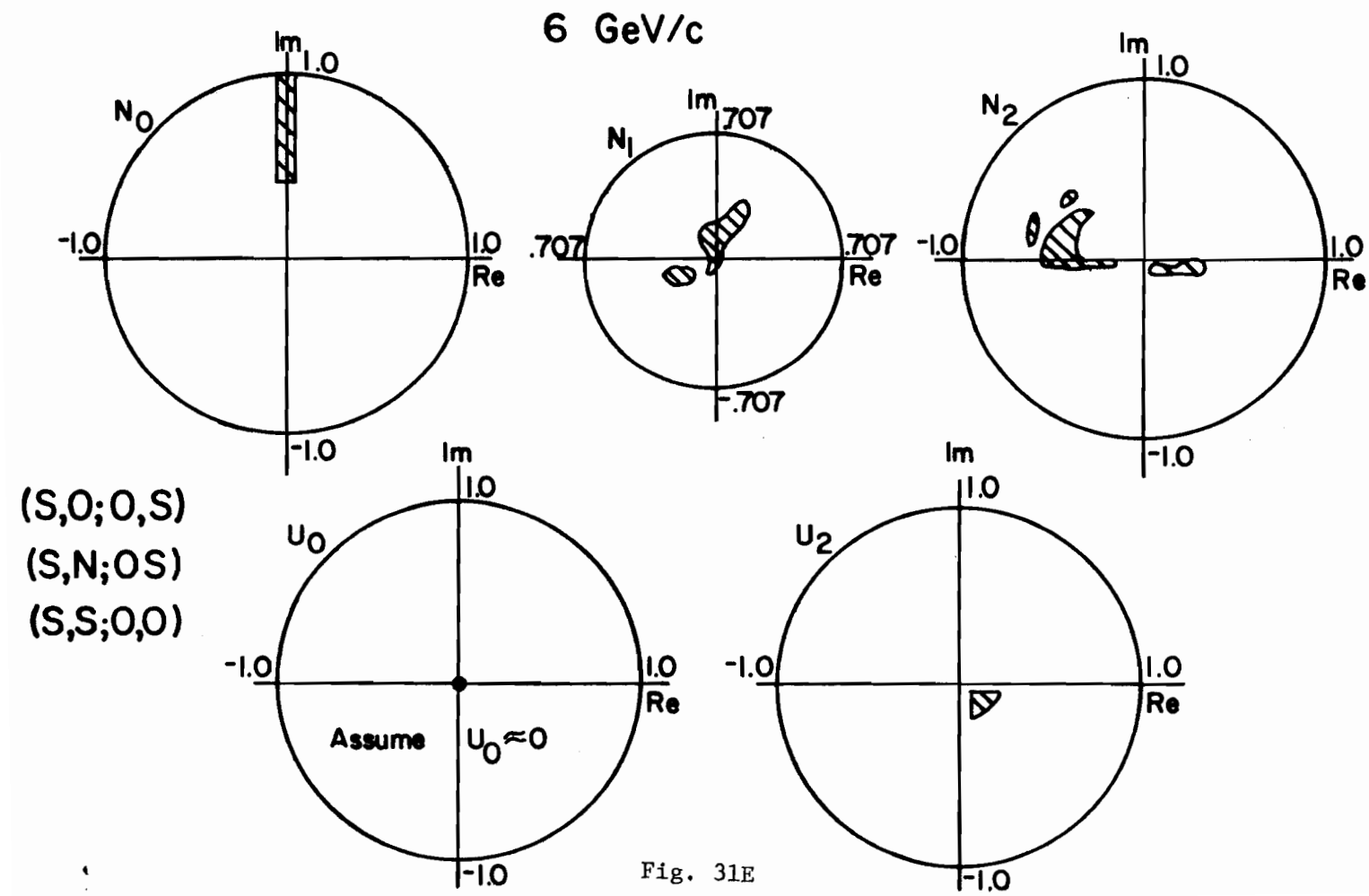

Fig. 31E